UPPSALA
UNIVERSITET

Digital Comprehensive Summaries of Uppsala Dissertations from the Faculty of Science and Technology 1208

Development and Multicolor Imaging Applications of Lanthanide-Based Luminescent Probes

ELIAS PERSHAGEN

ACTA
UNIVERSITATIS
UPSALIENSIS
UPPSALA
2014

ISSN 1651-6214
ISBN 978-91-554-9112-3
urn:nbn:se:uu:diva-236760

Dissertation presented at Uppsala University to be publicly examined in Magnelisalen, Stockholm University, Svante Arrhenius väg 16, Stockholm, Wednesday, 28 January 2015 at 10:00 for the degree of Doctor of Philosophy. The examination will be conducted in English. Faculty examiner: Professor Stéphane Petoud (Centre de Biophysique Moléculaire, CNRS).

Abstract

Pershagen, E. 2014. Development and Multicolor Imaging Applications of Lanthanide-Based Luminescent Probes. *Digital Comprehensive Summaries of Uppsala Dissertations from the Faculty of Science and Technology* 1208. 76 pp. : Acta Universitatis Upsaliensis. ISBN 978-91-554-9112-3.

The study of biological analytes in their native environment is a major challenge for biochemistry and molecular biology. Luminesce spectroscopy is well suited for this task due to its non-invasiveness, high spatial and temporal resolution, and high signal to noise ratio. This thesis describes the development and applications of Ln-based luminescent probes for detecting small molecules and enzymes. Specifically the probes presented are based on coumarin sensitizers coupled to a DO3A chelated Ln^{III} center. The 1st generation of these probes employ 7-OH coumarins, caged at the 7-O position (Chapter 2). By use of *p*-pinacolatoboron benzyl or *p*-methoxybenzyl cages, this design allowed the construction of ratiometric Eu^{III}-based probes capable of detecting the reactive oxygen species H_2O_2, NO and $ONOO^-$.

The second and third part of the thesis describes a further improvement of the design (Chapters 3 and 4). By employing caged coumarin *precursors* Eu^{III} and Tb^{III}-based probes were developed for a variety of different analytes (F^-, Pd^0, H_2O_2, β-galactosidase, β-glucosidase, α-mannosidase and phosphatase). Most of these probes displayed excellent turn-on responses when treated with their respective analytes. Furthermore they could be used for detecting multiple analytes simultaneously (Chapter 4). By use of one Eu-based and another Tb-based probe, the simultaneous detection of two analytes was possible. This could further be extended to simultaneous three analyte detection by the additional employment of an organic coumarin-based probe.

The last part of the thesis (Chapter 5) describes protocols for the rapid and efficient access to triazole-linked lanthanide-antenna complexes by use of the copper-catalyzed azide-alkyne cycloaddition reaction. For robust substrates, microwave heating at 100 °C enabled rapid (15-60 min) access to various lanthanide complexes, which could be isolated via simple precipitation. Using these conditions pure bi- and tri-homometallic lanthanide complexes could be prepared. A second protocol, for substrates carrying sensitive functionalities was also developed. The application of catalytic amounts of CuOAc, $BimPy_2$ ligand, and a large excess of NaAsc afforded a variety of lanthanide complexes, among them caged responsive probes, in moderate to good yields.

Keywords: Lanthanide, luminescent probe, multicolor

Elias Pershagen, Department of Chemistry - BMC, Physical Organic Chemistry, Box 576, Uppsala University, SE-75123 Uppsala, Sweden.

ISSN 1651-6214
ISBN 978-91-554-9112-3
urn:nbn:se:uu:diva-236760 (http://urn.kb.se/resolve?urn=urn:nbn:se:uu:diva-236760)

List of Papers

This thesis is based on the following papers, which are referred to in the text by their Roman numerals.

I Szíjjártó, C.,[†] Pershagen, E.,[†] Ilchenko, N. O., Borbas, K. E.
A versatile long-wavelength-absorbing scaffold for Eu-based responsive probes. *Chem. – Eur. J.* **2013**, *19*, 3099–3109. [†]These authors contributed equally.

II Pershagen, E., Nordholm, J., Borbas, K. E.
Luminescent lanthanide complexes with analyte-triggered antenna formation. *J. Am. Chem. Soc.* **2012**, *134*, 9832–9834.

III Pershagen, E., Borbas, K. E.
Multiplex detection of enzymatic activity with responsive lanthanide-based luminescent probes. *Angew. Chem. Int. Ed.* DOI: 10.1002/anie.201408560R1

IV Szíjjártó, C., Pershagen, E., Borbas, K. E.
Functionalisation of lanthanide complexes via microwave-enhanced Cu(I)-catalysed azide-alkyne cycloaddition. *Dalton Trans.* **2012***, 41*, 7660–7669.

Publications not included in the thesis:

V Pershagen, E., Borbas, K. E.
Designing reactivity-based responsive lanthanide probes for multicolor detection in biological systems. *Coord. Chem. Rev.* **2014**, *273–274*, 30–46.

Contributions

Paper **I**. Contributed to the synthetic work. Performed the RONS selectivity studies and the kinetic studies. Co-wrote the supplementary information.

Paper **II**. Performed the majority of the synthetic work and the NMR-studies. Co-wrote the supplementary information.

Paper **III**. Performed the majority of the synthetic work and all of the photophysical studies and probe testing. Wrote the majority of the supplementary information.

Paper **IV**. Performed the photophysical studies and HPLC and HR-ESI-MS characterization of the compounds. Minor contributions to the supplementary information.

Contents

Abbreviations

Abbreviations are used in agreement with the standards of the subject.[1] Non-standard abbreviations that appear in the thesis are listed here.

AIBN	Azobisisobutyronitrile
Asc	Ascorbate
B_2pin_2	Bis(pinacolato)diboron
$BimPy_2$	N-((1H-benzo[d]imidazol-2-yl)methyl)-1-(pyridin-2-yl)-N-(pyridin-2-ylmethyl)methanamine
Boc	tert-butyloxycarbonyl
Bpin	pinacolatoboron
CuAAC	Copper-catalyzed azide-alkyne cycloaddition
DIPEA	N,N-Diisopropylethylamine
DO3A	1,4,7,10-tetraazacyclododecane-1,4,7-triacetic acid
dppf	1,1′-Bis(diphenylphosphino)ferrocene
DTPA	Diethylene triamine pentaacetic acid
Fwhm	Full width at half maximum
HATU	O-(7-Azabenzotriazol-1-yl)-N,N,N′,N′-tetramethyluronium hexafluorophosphate
HEPES	2-(4-(2-hydroxyethyl)-1-piperazinyl)ethanesulfonic acid
LacZ	Part of the lac operone, encoding β-galactosidase
Ln	Lanthanide
Ms	Mesityl
n.d.	Not determined
NBS	N-bromosuccinimide
PeT	Photoinduced electron transfer
PTP1B	Protein tyrosine phosphatase 1B
q	Hydration state
RET	Resonance energy transfer
RNS	Reactive nitrogen species
RONS	Reactive oxygen and nitrogen species
ROS	Reactive oxygen species
rt	Room temperature
S/N	Signal to noise ratio
TBAF	Tetrabutylammonium fluoride

TBTA	Tris((1-benzyl-1H-1,2,3-triazol-4-yl)methyl)amine
Tf	Trifluoromethanesulfonate
TFA	Trifluoroacetic acid
THPTA	3,3′,3″-(4,4′,4″-(Nitrilotris(methylene))tris(1H-1,2,3-triazole-4,1-diyl))tris(propan-1-ol)
TIPS	Triisopropylsilyl
TMS	Trimethylsilyl
U	Unit – measure of enzyme activity
τ	Luminescent lifetime
Φ_L	Quantum yield of luminescence

1. Introduction

Human curiosity has driven the invention of tools that enable us to see beyond the limits set by our senses. These tools span from telescopes, for viewing distant stars and galaxies, to particle accelerators, for observing the fundamental building blocks of nature. In between these extremes, and at the heart of chemistry, are molecules, and a variety of techniques have been developed to probe their interactions. However, singling out and studying selected processes amongst a large number of competing ones is still a challenging task indeed. Although difficult, it is a vital challenge to overcome if we are ever to understand the workings of complex systems such as cells, where millions of reactions occur every second.[2]

One powerful approach to tackle this problem, known as luminescence spectroscopy, takes advantage of the interactions of light with molecules. Molecules that interact efficiently with light by absorbing and emitting photons are called luminophores, and often contain aromatic or highly conjugated systems.[3,4] In order to take advantage of the interaction of a luminophore with light to study a selected event, the luminophore needs to respond to the event in question. Such responsive luminophores are usually called luminescent probes and a large amount of research has been focused on finding efficient ways of making luminophores respond to selected events.[5]

This thesis concerns the development of such tools, namely luminescent lanthanide-based probes. The thesis covers both the construction of the probes as well as their applications in detecting biologically relevant small molecules and enzymes. The first part of the introduction aims to give a brief overview of the challenges of studying biological systems while the second part deals with the general principles behind luminescent probes in general and lanthanide based probes in particular.

1.1 The challenge

Cells are often considered the most basic unit of life, yet they are vastly complex, orchestrating millions of interconnected reactions every second.[2] Untangling these interactions is a major challenge for biochemistry and molecular biology. The value in doing so lies in part in the better understanding of healthy and diseased states, knowledge that in the long run can be used in the development of new drugs or the prevention of illnesses.

A number of complementary techniques exist to study cells and cellular components.[2,6] Perhaps the most direct way of gaining understanding of a selected analyte's role is to visualize it in live cells (preferably while simultaneously looking at interconnected components). As noted above this thesis concerns the development of luminescent lanthanide-based probes that can aid in such study of cellular components. Specifically, the analytes we have focused on are phosphatases, glycosidases and reactive oxygen and nitrogen species. This section aims to describe our motives behind choosing these analytes by briefly discussing their biological roles.

Much of the cell's functions are regulated by signaling networks. Signaling is the transfer of information towards and within the cell, and enables it to respond to specific stimuli. The end result of a signaling cascade is often phosphorylation or dephosphorylation of some protein, which alters its activity and in turn the activity of the cell.[7] Protein phosphorylation is catalyzed by kinases and phosphorylases, while dephosphorylation is catalyzed by phosphatases. Dysregulation of phosphatase activity has been linked to diabetes, obesity and cancer.[8]

Certain phosphatases can be regulated by reactive oxygen or nitrogen species (RONS).[9] RONS are small oxidizing molecules with various biological functions and include $^{\bullet}OH$, $^{1}O_2$, $O_2^{\bullet-}$, H_2O_2, HOCl, NO and $ONOO^-$ among others. RONS are not only regulators of protein function by redox signaling. High levels of RONS produce oxidative stress, which is implicated in various disease states such as cancer and Parkinson's and Alzheimer's diseases.[10]

Besides protein phosphorylation, protein glycosylation can also produce structural modifications of proteins and as such be part of signaling cascades.[11] In addition, glycosides are critical for cell-cell and cell-pathogen recognition, and as such play a role in the immune system.[11] Glycosylation is mediated by glycosidases and glycosyltransferases.[11]

A key feature of signal transducing systems is the ability of the system to respond to multiple signals by a unified response. There is considerable crosstalk between different signaling pathways.[7] This interconnectedness means it is often informative to study several components of the system simultaneously, something which is discussed in Chapter 4.

As noted above, our approach for detecting such components is to use lanthanide-based luminescent probes. The remaining parts of the introduction discuss the principles of such probes.

1.2 Interaction of light with molecules

Light, or electromagnetic radiation, can be described both as a particle (photon) and as an oscillating field with an electric and a magnetic component. While physicists often refer to all electromagnetic radiation as light, in this

thesis the word *light* is reserved to electromagnetic radiation in the region of the spectrum stretching from ultraviolet (UV) to near-infrared (NIR).

Light within this frequency region can induce electronic transitions in molecules. For this to occur, the molecule must at least transiently possess a dipole oscillating at the same frequency as the light (this, however, should not be confused with the permanent dipoles of certain molecules).[12] However, due to symmetry considerations, not all electronic transitions are allowed.

When absorption occurs in a molecule, it is excited from its ground state to an excited state. This usually means promoting an electron from the highest occupied molecular orbital (HOMO) to the lowest unoccupied molecular orbital (LUMO). When an electron is promoted to a higher energy orbital its spin remains unchanged and consequently the multiplicity of the molecule will be unchanged. For most organic molecules, which are closed shell singlets in their ground state, both states are singlet states (denoted S_0 for the ground state and S_1 for the first excited state). Each electronic state is divided into a number of vibrational sublevels.[12] To illustrate the various photophysical processes that can occur within a molecule a Jablonski diagram is often used (Figure 1).[13]

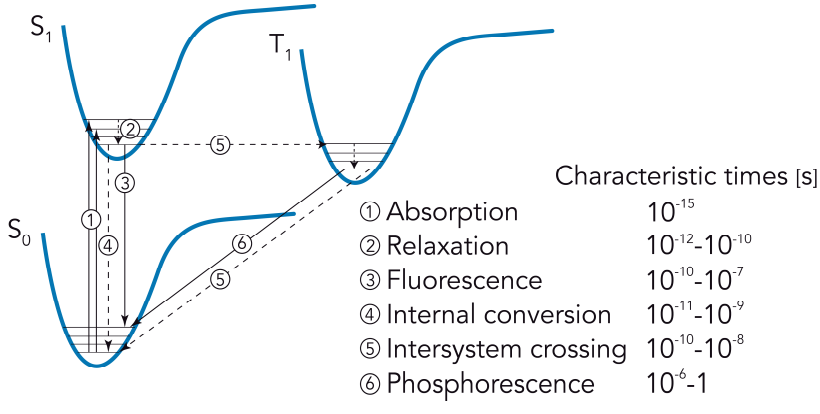

Figure 1. Jablonski diagram depicting the most common photophysical processes.[14]

At room temperature most molecules are in their electronic ground state S_0, with nuclei at their equilibrium distance to each other. Following absorption and promotion of an electron to an excited state, the electron density is redistributed within the molecule. Because nuclear motion is much slower than electronic transitions, the nuclei will not immediately respond to this new electronic environment. As a result, excitation normally occurs to a higher vibrational sublevel of the excited state (Figure 1, 1). This is known as the Franck-Condon principle.[15]

Following absorption, the molecule can relax down to the lowest vibrational sublevel of the excited state by dissipating some of the energy internally through conformational changes, or externally to surrounding molecules (Figure 1, 2). If such a relaxation occurs all the way to the ground state it is referred to as internal conversion (Figure 1, 4). However, because of the much larger energy gap between the S_1 and S_0 state, the surrounding molecules may be unable to accept the energy required for this transition. Instead, return to the ground state can occur with the simultaneous release of a photon (Figure 1, 3), this process is known as fluorescence.[12] In addition, a molecule in an S_1 state can undergo an interconversion to a triplet state (denoted T_1, Figure 1, 5). Such a process, known as intersystem crossing, is formally forbidden but can occur if the singlet has an isoenergetic triplet state,[16] and a mechanism exists to make this transition partially allowed, such as spin-orbit coupling.[17] Return from an excited triplet state to the ground singlet state is known as phosphorescence (Figure 1, 6). Since phosphorescence, like intersystem crossing, is spin forbidden it is much slower than fluorescence (with characteristic lifetimes in the order of ms−s compared to ns for fluorescence).

In certain species, such as transition metal or lanthanide complexes the nature of the excited state can be unclear.[14] In such cases the term luminescence, which covers both fluorescence and phosphorescence, can be used to refer to the emission. Consequently, the term luminophore is used to refer to species which display luminescence and the more narrow terms fluorophore and phosphor are used for species that emit light by fluorescence and phosphorescence, respectively.

1.3 Experimental study of luminescence

An instrument often used to study luminescent compounds is the spectrofluorometer. This is a device that can excite samples and record their emission (Figure 2a). Usually a cuvette is loaded with a liquid sample and placed in the sample holder. The sample is then excited by a light source and the emission from the cuvette is recorded at a 90° angle to minimize interference from the excitation source. The light source is often a xenon lamp which emits at all wavelengths between 250−1000 nm (although not at the same intensities). Before the excitation light reaches the sample it is passed through a monochromator which selects out the wavelength chosen by the operator (by the use of prisms, diffraction gratings or filters). The emission from the sample then passes through another monochromator (in order to decompose the spectrum of the emitted light) before reaching the detector.[18]

Most spectrofluorometers can record both excitation and emission spectra. An emission spectrum is a plot of the emission intensity vs. wavelength using a fixed *excitation* wavelength. Conversely, an excitation spectrum is a

plot of the emission intensity vs. wavelength using a fixed *emission* wavelength and scanning the excitation wavelength. A molecule's emission spectrum is usually an approximate mirror image of its excitation spectrum, which in turn, closely resembles its absorption spectrum.[14,18] Notable exceptions to the mirror image rule are molecules that undergo resonance energy transfer (RET), and certain transition metal and lanthanide complexes.[18]

Some spectrofluorometers are capable of time gating the sample emission. This can be achieved in various ways, the result being that the emission can be recorded a fixed time after excitation, in contrast to the continuous detection employed in steady state spectroscopy (Figure 2b). Time resolved spectroscopy can be used to gain additional information from a sample other than just its emission and excitation spectrum, such as luminescence lifetimes. Additionally the technique can be used to increase the signal to noise ratio (S/N) in samples containing fluorophores with shorter lifetimes than the molecule of interest (see below).[18]

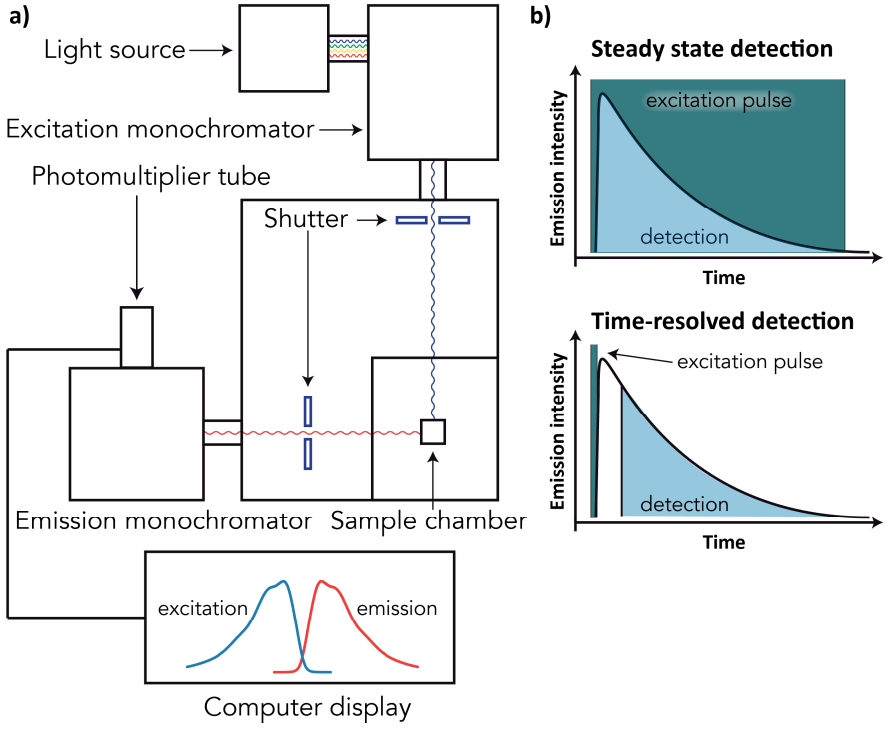

Figure 2. a) Schematic drawing of a spectrofluorometer. b) Illustration of the difference between steady state and time-resolved detection.

Other instruments commonly employed in luminescence spectroscopy are luminescence plate readers and microscopes. While these instruments are not as sensitive as spectrofluorometers, they offer complementary capabilities. These include the capacity for high-throughput measurements (fluorescence

plate readers) and the ability to study localized processes in live cells (fluorescence microscopes).[18]

Luminescence spectroscopy is a very sensitive technique, so sensitive in fact, that it can be used to detect single molecules in solution.[19] The sensitivity stems from the ability to detect signals over an essentially zero background.[14] This means that extremely sensitive detectors can be used that amplify very weak signals. Luminescence spectroscopy can also provide very high temporal and spatial resolution. Super-resolution microscopy (often called nanoscopy) has pushed the boundary of spatial resolution beyond the diffraction limit of light.[20]

Despite the very high sensitivity of the technique, without efficient luminophores the information that can be gained is limited. Some important properties that determine the usefulness of a luminophore for spectroscopy are summarized below.

1.3.1 Brightness

The brightness (B) of a luminophore is the product of its absorption coefficient (ε) and luminescence quantum yield (Φ_L). The absorption coefficient is the measure of a molecule's ability to absorb light at a certain wavelength. The efficiency of absorption is expressed as the molar absorption coefficient ε in the Beer-Lambert law:

$$A = \varepsilon l c$$

where A is the absorbance at the specific wavelength measured, l the path length, and c the concentration of the luminophore. The quantum yield of luminescence (Φ_L) is the number of emitted photons per number of photons absorbed. Alternatively, the quantum yield of luminescence can be expressed in terms of relative rates:

$$\Phi_L = \frac{k_r}{k_r + k_{nr}}$$

where k_r and k_{nr} are the summed rate constants for radiative and non-radiative decay, respectively. High brightness is important because it reduces the amount of luminophore needed for spectroscopy. The brightness of some natural and synthetic fluorophores are plotted in Figure 3.

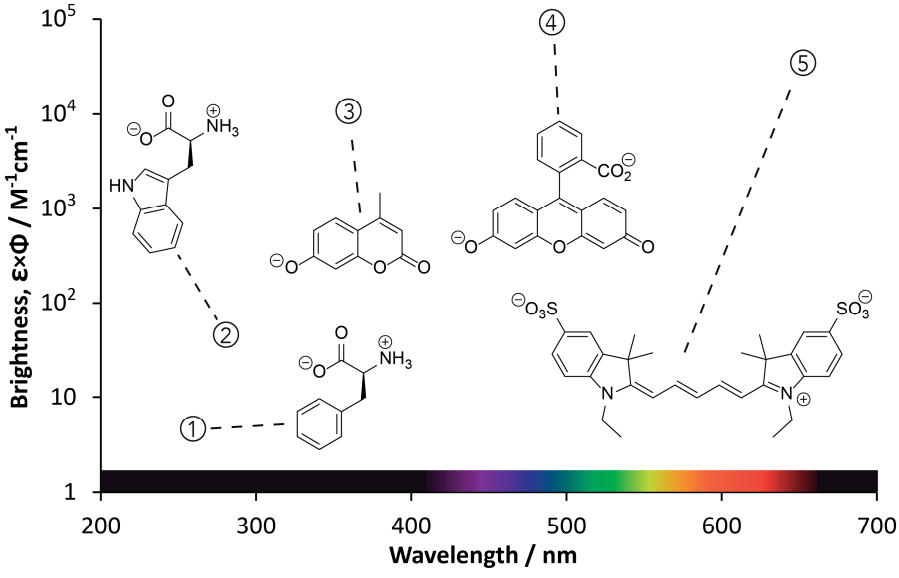

	Φ_L	ε ($M^{-1}cm^{-1}$)
① Phenylalanine	0.024	200
② Tryptophan	0.13	348
③ 4-Methylumbelliferone	0.63	17 000
④ Fluorescein	0.95	93 000
⑤ Cyanine 5	0.18	200 000

Figure 3. The brightness of some fluorophores plotted against their wavelength of maximum absorbance.[5b]

1.3.2 Stokes shift

The Stokes shift is the wavelength difference between the maxima of the lowest energy absorption and the emission.[3,21] The Stokes shift occurs as a consequence of the relaxation down the vibrational sublevels of the excited state. As a result, the emitted light will have lower energy (longer wavelength) than the absorbed light (Figure 4). This phenomenon was first observed by G. G. Stokes by looking at a solution of quinine sulfate through a yellow filter (a glass of wine).[22] A large Stokes shift is desirable since it minimizes luminophore self-quenching as well as interference from excitation light (by scattering) in the detection channel.

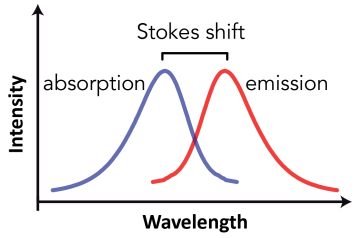

Figure 4. Illustration of the Stokes shift.

1.3.3 Additional requirements for bioimaging

Studying biological systems puts additional requirements upon the luminophore. Certain biomolecules are themselves fluorophores and these can interfere with the measurement by absorbing and emitting light. Fluorescent biomolecules include tyrosine ($\lambda_{abs}/\lambda_{em}$ 275 nm/303 nm, ε = 1500 M^{-1} cm^{-1}), tryptophan ($\lambda_{abs}/\lambda_{em}$ 280 nm/348 nm, ε = 6300 M^{-1} cm^{-1}), NADH ($\lambda_{abs}/\lambda_{em}$ 340 nm/435 nm, ε = 6200 M^{-1} cm^{-1}) and the flavins ($\lambda_{abs}/\lambda_{em}$ 450 nm/530 nm, ε = 12200 M^{-1} cm^{-1}).[5b] In tissue, absorbance from hemoglobin and oxyhemoglobin is high at wavelengths < 600 nm.[23] Since most of the biological fluorophores absorb and emit light in the UV- or near UV-region, one way to minimize the interference from these is to use luminophores that absorb and emit at longer wavelengths. The NIR region is especially well suited for this as biological media is highly transparent to light at these wavelengths. However, at wavelengths > 950 nm absorbance from water and lipids starts to interfere. Hence the wavelength region 650−950 nm is often referred to as the "biological window" of luminescence spectroscopy.[23-24]

Another way to increase the S/N is to use luminophores with long excited state lifetimes. The luminescent lifetime (τ_L) is the average time a compound exists in the excited state.[18] It is expressed as the inverse of the combined radiative and non-radiative deactivation processes. Most biological fluorophores have lifetimes on the order of nanoseconds, thus by employing luminophores with longer lifetimes and using time gating, the interfering emission from these can be removed (Figure 5).

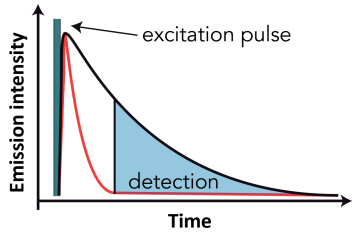

Figure 5. Illustration of how time-resolved detection can be used to increase S/N. Detection is initiated only after background fluorescence (red) has ceased.

1.4 Responsive luminescent probes

One of the major applications of luminescence imaging is the study of analytes in biological systems. However, many analytes are not themselves luminescent. In such cases indirect detection can still be possible by placing the emission of another, luminescent molecule, under the control of the analyte of interest.

A molecule that reports on an analyte by a change in its light emission is called a responsive luminescent probe. Most often this change is either an increase (turn-on) or decrease (turn-off) in the emission intensity of the probe (Figure 6a).[25] Such a change in brightness is the most straightforward luminescence parameter to measure, and by far the most employed response in luminescent probes. However, a drawback with measuring emission intensity changes at a single wavelength is the dependence of such measurements on luminophore concentration and instrument excitation power. This can make analyte quantification difficult, especially in environments such as cells where the probe concentration cannot be expected to be uniform. Some luminescent probes respond by a simultaneous emission increase and decrease, at different wavelengths (Figure 6b). The ratio of the intensities at these different wavelengths is independent of probe concentration and as such provides a more robust readout. Another parameter that is (most often) independent of probe concentration is the luminescence lifetime, and this is exploited in some luminescent probes (Figure 6c).

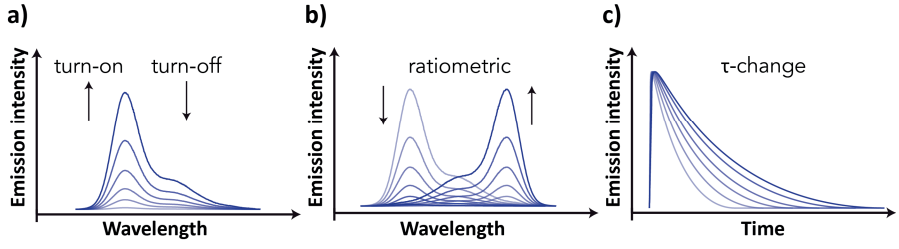

Figure 6. Illustration of different luminescence responses.

A large amount of research has been devoted to finding efficient ways of making luminophores analyte responsive.[26] Broadly, these approaches can be divided into two categories based on their detection mechanism: recognition-based and reaction-based.[27] Recognition-based probes rely on reversible, non-covalent interactions between the analyte and the probe. Since binding of the analyte is reversible such probes can report on fluctuations in analyte concentrations. Reaction-based probes contain a moiety that chemoselectively reacts with the analyte of interest to produce the photophysical change in the probe. In general, reaction-based probes offer greater selectivity and larger spectroscopic changes compared to recognition-based probes. However, reaction-based probes have the inherent disadvantage that fluctua-

tions in analyte concentration cannot be monitored. A selection of different responsive probes is shown in Scheme 1.

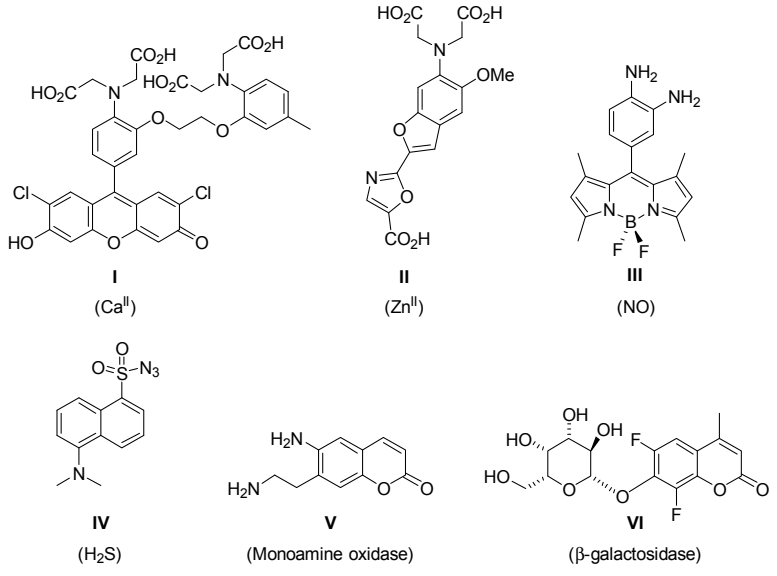

Scheme 1. Examples of some luminescent probes used for in vivo imaging. ***I****[28] and* ***II****[29] are based on non-covalent recognition, while* ***III-VI****[30] are reaction-based. The analyte for each probe is given in parentheses.*

In addition to the photophysical demands of the luminophore described in the previous section, probes for *in vivo* use need to meet further requirements. These include high water solubility, high photostability and low toxicity. Furthermore, the interaction with the analyte should be highly specific and proceed with reasonable kinetics in water.[5a,31]

The interconnectedness of biological processes means it is often informative to study two or more analytes simultaneously. However, the small Stokes shifts and broad emission bands of commonly employed organic luminophores can make this challenging. The careful choice of excitation and emission filters or the use of spectral unmixing algorithms can sometimes overcome problems of overlapping emission bands.[32] However, for convenience, a single excitation wavelength and well separated emission bands are desirable. The lanthanides provide some attractive features in this respect, such as large Stokes shifts[33] and narrow emission bands. The remainder of the introduction is devoted to discussing some key properties and uses of these elements.

1.5 Introducing the lanthanides

The chemistry of the lanthanides began in 1751 when the Swedish mineralogist A. F. Cronstedt discovered a mineral which was later shown to contain a mixture of lanthanides.[34] Today the term lanthanide (Ln) is usually meant to refer to the elements shown in Figure 7. However, there is no general agreement and sometimes only Ce-Lu are included.[35] Despite being commonly known as the "rare earths" the lanthanides, with the exception of the radioactive Pm, are actually not rare.[34]

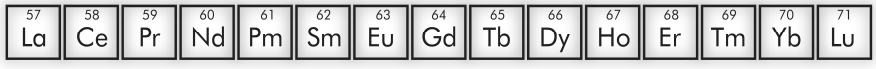

Figure 7. The lanthanides.

The chemistry of the Lns is mostly governed by their +III oxidation state and largely resembles that of the group II elements.[36] The 4f orbitals are well shielded by the 5s and 5p orbitals and as a result they play little role in bonding. Bonding in Ln compounds is thus almost exclusively ionic, hence the coordination number and geometry of Ln complexes is mainly determined by steric factors. The coordination number varies depending on the size of the ligands but is usually between 6−12, in the aquo ions $[Ln(H_2O)_n]^{3+}$ this number is 9 for the earlier Lns La^{III}-Eu^{III} and 8 for Dy^{III}-Lu^{III}.[35] The trivalent Lns are hard ions and consequently prefer anionic ligands of high electronegativity such as oxygen and fluoride donors.[36]

With the exception of La^{III} and Lu^{III}, the trivalent Lns are luminescent and a large portion of their commercial applications take advantage of this property. Lanthanides are used in Euro banknotes to prevent counterfeiting, and certain luminescent lights use Ln-doped phosphors.[37]

1.5.1 Lanthanide luminescence

The photophysical properties of the Ln^{III} ions arise from transitions between different energy levels of the 4f orbitals. Due to the shielding of the 4f orbitals these energy levels are mostly unaffected by the chemical environment surrounding the metal. As a result they produce very characteristic and narrow emission peaks (Figure 8). The 4f transitions are formally forbidden and as a consequence the free Ln^{III} ions have low absorption coefficients (typically $< 3\ M^{-1}\ cm^{-1}$) and long excited state lifetimes (up to ms).[38]

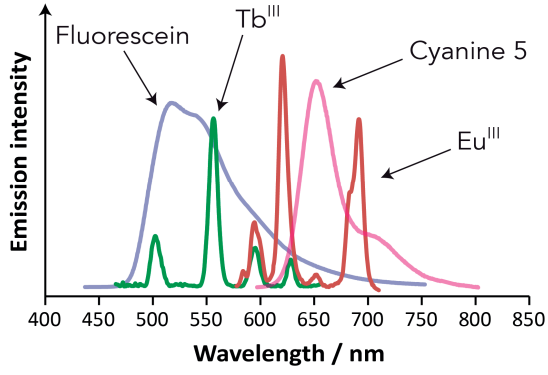

Figure 8. Comparison of the emission spectra of Tb and Eu to those of the commonly used fluorophores Fluorescein and Cyanine 5.

The brightness of the different Lns varies considerably and this is largely due to differences in their intrinsic quantum yields (Φ_{Ln}). The quantum yield is related to the ease with which the excited state can be depopulated by non-radiative processes. The smaller the gap between the emissive state of the Ln and its highest ground state, the easier this will be. Gd is the most luminescent, however its emission is in the UV (310 nm) and it is seldom used for its luminescent properties.[39] The visible emitting Eu and Tb provide a balance between high intrinsic quantum yields and long emission wavelengths.

In water, quenching of the Ln excited state by high-energy O-H vibrations is a major deactivation pathway. One way to protect the Ln^{III} ion from this is by employing a multidentate chelating ligand. Commonly employed ligands include polyaminocarboxylates such as DTPA and DO3A derivatives (Scheme 2). These provide high kinetic and thermodynamic stabilities and shield off most of the Ln-coordinating water molecules.[40]

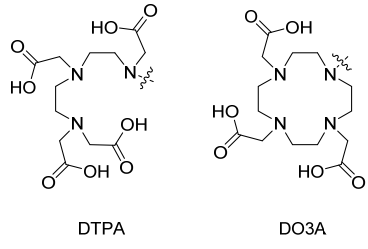

Scheme 2. Structure of DTPA and DO3A.

A number of equations have been proposed that enable assessment of the hydration state (q) of the Ln. Most of these equations consider the differences in lifetimes of the Ln in H_2O and D_2O and work under the assumption that vibrational O-D quenching of the Ln excited state is negligible. For Eu and Tb the relationship has the following form:[41]

$$q = A_{\mathrm{Ln}}\left(\frac{1}{\tau_{\mathrm{H_2O}}} - \frac{1}{\tau_{\mathrm{D_2O}}} - B_{\mathrm{Ln}}\right)$$

A_{Ln} and B_{Ln} are Ln specific values added to correct for the contributions of outer sphere water molecules to the deactivation of the excited state. Their values are $A_{Eu} = 1.2$, $A_{Tb} = 5$, $B_{Eu} = 0.25 + 0.07x$, $B_{Tb} = 0.06$, and x is the number of exchangeable N-H oscillators. Calculated values have an uncertainty of ~0.3 and must be interpreted with some caution.[41a,42]

However, a strong chelate that prevents water coordination is not enough to produce bright Ln complexes. The very low absorption coefficients of the Lns make direct excitation difficult. The Ln excited state can be reached by other means though, namely by energy transfer from another excited molecule (often an organic chromophore). This phenomenon, which was first observed by Weissman in the 1940s, is called luminescence sensitization or the antenna effect and consequently the organic chromophore is often referred to as sensitizer or antenna.[43] Coupling an organic chromophore to a Ln complex can increase the brightness by several orders of magnitude. A selection of chromophores which have been employed as Ln-sensitizers are shown in Scheme 3.

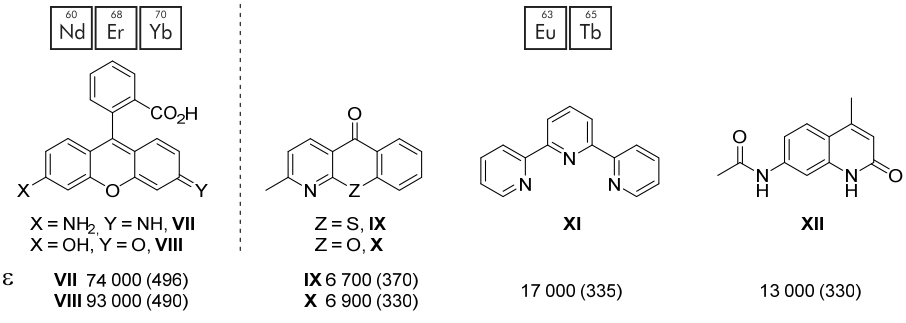

Scheme 3. A selection of chromophores which have been employed as Ln-sensitizers. The selection is limited to chromophores that have been incorporated into Ln-based probes. ***VII****[44] and* ***VIII****[45] have been used to sensitize Nd, Er and Yb, while* ***IX****,[46]* ***X****,[46]* ***XI****[47] and* ***XII****[48] can sensitize Eu and Tb. ε values are reported in* M^{-1} cm^{-1} *with the wavelength of the maximum absorption (in nm) in parentheses. Linkers and Ln-chelates have been removed for clarity.*

A model of lanthanide sensitization considers the energy flow from the sensitizer's excited singlet or triplet state to the Ln excited state (Figure 9).[49] The sensitization efficiency (η_{sens}) depends on the energy transfer efficiency (η_{et}) and, in the case of triplet sensitization, on the efficiency of $S_1 \rightarrow T_1$ intersystem crossing (η_{ISC}). In addition to the singlet and triplet sensitization pathways, other energy transfer processes such as ligand to metal charge transfer (LMCT) may operate. Triplet sensitization is often invoked simply on the basis of the long lifetime of the antenna triplet state. However, the

actual pathway in operation depends on the differences in relative rates and is not easily modelled (consideration of 20−30 rate constants may be necessary in certain cases[49a]).

The brightness (B) of a Ln-antenna complex can be expressed as a product of the antenna absorption coefficient ($\varepsilon_{antenna}$), sensitization efficiency (η_{sens}) and the intrinsic quantum yield of the Ln (Φ_{Ln}):

$$B = \varepsilon_{antenna}\eta_{sens}\Phi_{Ln}$$

As absorption coefficients for organic chromophores are several orders of magnitude larger than for the free Ln^{III} ions, even very inefficient sensitization can produce large increases in brightness.

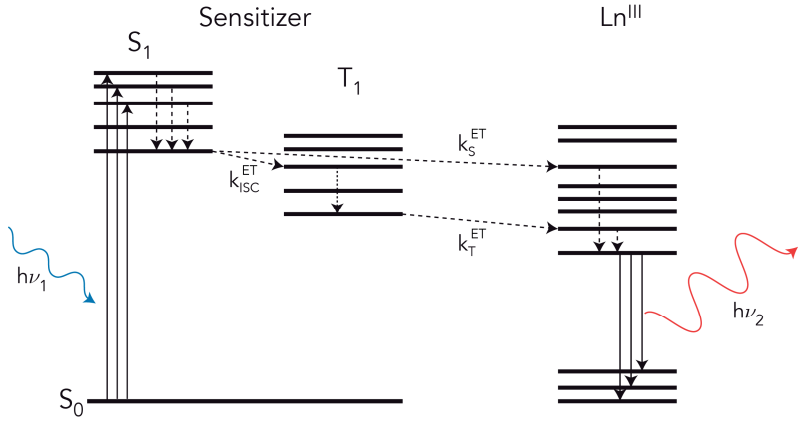

Figure 9. Simplified Jablonski diagram showing the energy flow from a sensitizer to a lanthanide. Energy back transfer processes have been omitted for clarity.

The choice of sensitizer is limited to those with a triplet state well above the Ln emissive state. This energy difference should be at least 3000 cm^{-1} in order to minimize energy back transfer from the Ln to the sensitizer.[50,49b,c] This means that antennae for Eu and Tb are limited to those which absorb at wavelengths below 430 and 400 nm, respectively.

1.5.2 Lanthanide-based luminescent probes

The lanthanides have found widespread use as emitters in responsive luminescent probes. Lanthanide-based probes provide a number of features not seen in purely organic probes such as long excited state lifetimes (up to ms compared to ns), large Stokes shifts[51] (hundreds of nm compared to ~10 nm) and narrow emission bands [full width at half maximum (fwhm) of ~10 nm compared to ~100 nm]. Although Ln-based probes often do not compare

well in terms of brightness, for many applications a high S/N is more important. In this respect the Ln-based probes provide a clear advantage. Their long excited state lifetimes enable time-resolved detection which can greatly increase the S/N *in vivo*. In addition, the narrow emission bands and large Stokes shifts facilitate multicolor detection of several Lns.[52]

A number of ways exist for rendering Ln-based probes analyte responsive. To achieve this, advantage can be taken of any number of the factors governing the brightness of Ln-antenna complexes. The need for an organic chromophore for efficient access to the Ln excited state means that many of the design strategies for rendering fluorescent probes analyte responsive can also be applied to Ln-based probes. Examples in this area include analyte triggered modulation of PeT quenching, analyte triggered phenol or aniline uncaging and analyte triggered antenna formation.[39,53] Other approaches such as analyte displacement of Ln-coordinated water molecules[46a,54] and analyte induced modulation of the Ln-antenna distance[55] have also been used.

Employing these strategies, a large number of luminescent Ln-based probes have been developed targeting a wide variety of analytes. Examples include pH,[56] metal ions,[55a,57] RONS,[55b,58] and other biologically relevant species.[46a,54a,59] Selected examples are shown in Scheme 4.

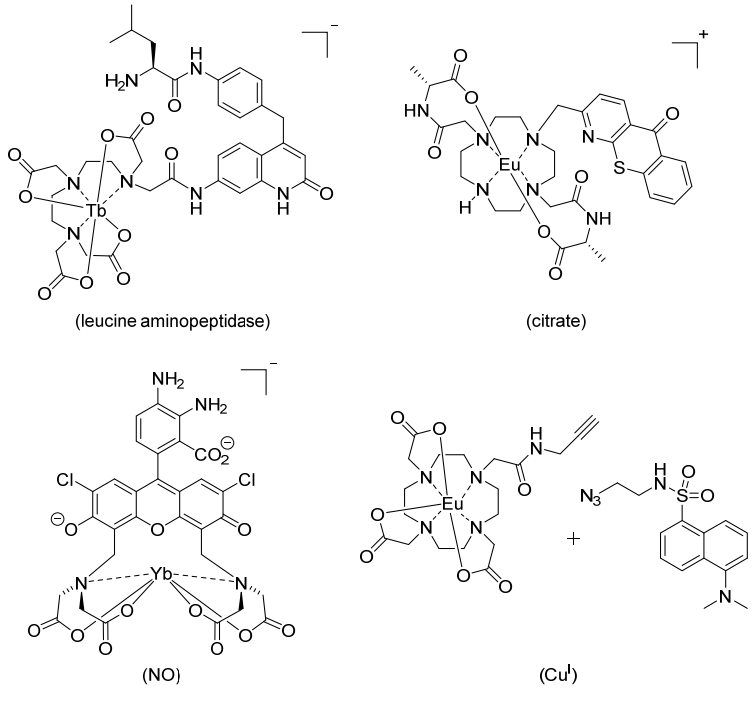

Scheme 4. Selected examples of Ln-based responsive probes. The analyte for each probe is given in parentheses.[45a,55a,59a,e]

2. A versatile long-wavelength-absorbing scaffold for Eu-based responsive probes (paper I)

The inertness of biological media to NIR light has directed considerable research focus into finding sensitizers for the NIR emitting Lns.[44-45,60] Of the lanthanides Yb, Nd, Sm and Er emit in the NIR region, and responsive probes incorporating Yb and Nd have been reported.[45c-f,61] Although Yb and Nd have attractive NIR emission, as a result of their small energy gap, these Lns are exceedingly sensitive to non-radiative deactivation leading to low intrinsic quantum yields.[38-39]

The visible-emitting Tb and Eu provide a compromise between long emission wavelengths and high brightness, and as a consequence these have been most frequently employed in responsive Ln-based probes. Chromophores for Eu and Tb are limited to those which absorb below 430 and 400 nm, respectively.[38,62] Given the damaging effects of high energy UV-light to biomolecules, there is good reason to find antennae with as red shifted absorption as possible for these Lns.

This work was carried out to investigate coumarin sensitized Eu complexes for reactivity-based analyte detection. It is well established that the absorption and emission spectra of coumarins are sensitive to substitution of the 7-position, with electron donating substituents affecting a red shift of the absorption. A literature survey comparing 7-O-alkylcoumarins to the corresponding phenolates showed that the absorption is red-shifted from 330−360 nm to 370−410 nm when going from the alkyl to the phenolate.[63] Thus caging the 7-O-position could be a viable approach for constructing ratiometric probes, as analyte triggered uncaging would lead to a red shift in absorption. To explore the feasibility of this idea we decided to develop probes for reactive oxygen and nitrogen species (RONS).

2.1 Results

A well-established H_2O_2 reactive moiety is the pinacolatoboron (Bpin) group, and as such we decided to incorporate it as a cage in our probes.[64] We decided to install it both directly to the coumarin (**4**) as well as via a *p*-

benzyl linker (**2a**) (Scheme 5). Additionally, the coumarins **2b-d** were prepared. We were hopeful that by altering the electron density of the benzyl moiety we would find caging groups which could selectively be cleaved by another RONS.

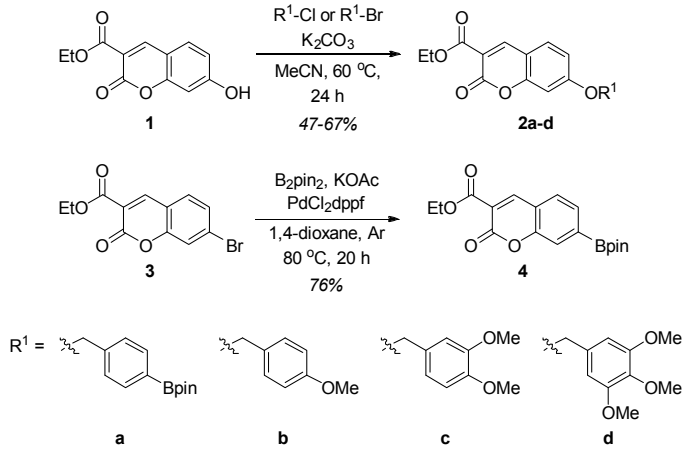

*Scheme 5. Synthesis of the caged coumarins **2a-d** and **4**.*

The *p*-benzyloxy linker employed in the caging groups is a well-established self-immolative linker.[65] Following initial uncaging, the formed *p*-tolylphenolate has been shown to cleave spontaneously, eliminating *p*-quinone methide (Scheme 6).[66]

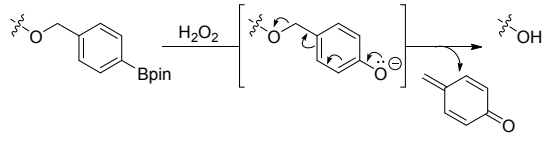

Scheme 6. Mechanism of quinone-methide elimination.

Before coupling these caged coumarins to Ln complexes we first wanted to probe their reactivity. We thus treated methanolic solutions of **2a-d** with various RONS (H_2O_2, $O_2^{\bullet-}$, $HO^{\bullet}$ and NO_2^-) and observed the resulting absorption changes. As expected, boronate cage **2a** reacted with H_2O_2, as evidenced by a decrease in absorption at 332 nm and an increase at 387 nm. While neither of the RONS tested affected the spectrum of **2c** and **2d** appreciably, exposure of **2b** to $O_2^{\bullet-}$ resulted in a decrease in absorption at 332 nm and the slow emergence of a new peak at 447 nm. Based on these data we decided to incorporate **2a-b** and **4** into Eu complexes.

The synthesis of the Eu complexes is shown in Schemes 7 and 8. Coumarin **5** was coupled with the amine equipped DO3A derivatives **6Et** or **6*t*-Bu** in a HATU mediated coupling (Scheme 7). The hydroxyl group of the cou-

marin in **7Et** was then alkylated with the benzyl bromide **a** or **b** to afford the caged coumarin **10a-b**. Basic ethyl ester cleavage, followed by Eu complexation in MeOH yielded the Eu complexes **Eu12a-b**. The uncaged reference compound **Eu9** was prepared from **7*t*-Bu** by acidic *t*-butyl ester cleavage followed by Eu complexation in MeOH.

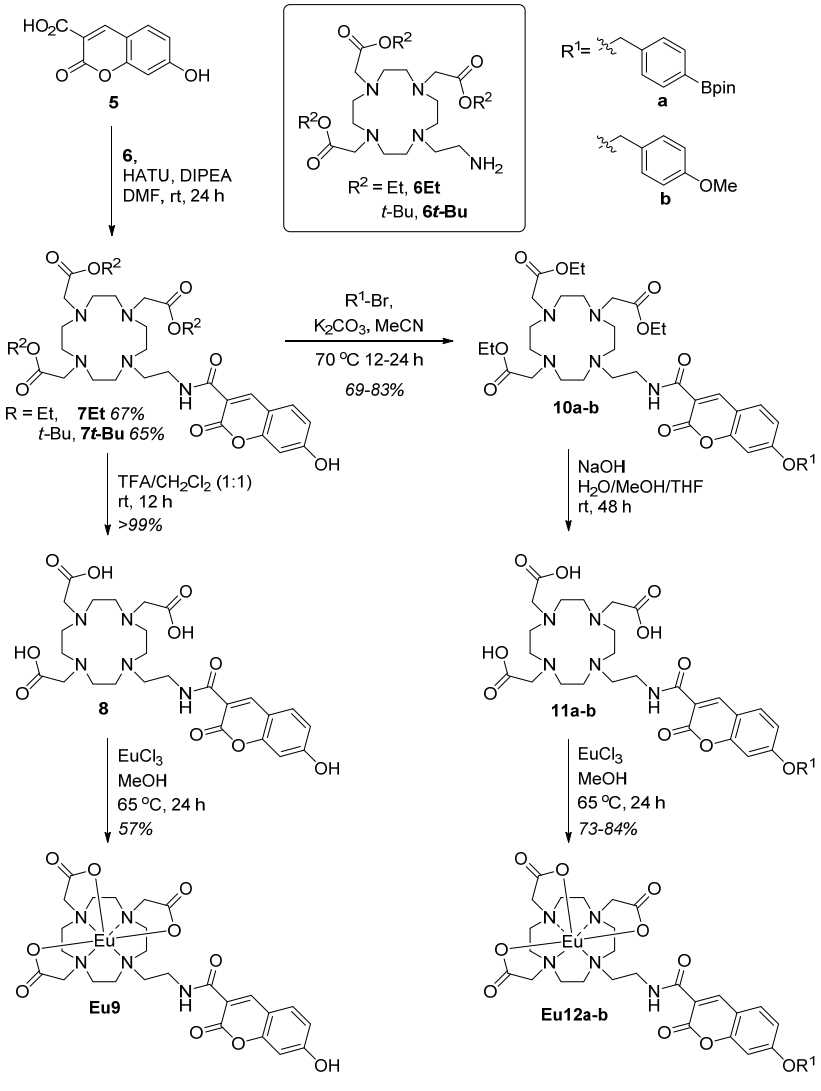

*Scheme 7. Synthesis of **Eu9** and **Eu12a-b**.*

In addition to these probes, **Eu19** was also synthesized (Scheme 8). The 7-Bpin coumarin **16** was prepared in four steps from **3**. The ethyl ester of **3** was first converted to its corresponding *t*-butyl ester derivative **14** by basic hydrolysis of **3** in a MeOH/H_2O mixture followed by $SOCl_2$ mediated for-

mation of the *t*-butyl ester **14**. Miyaura borylation, followed by *t*-butyl ester cleavage furnished the 7-Bpin coumarin **16** in 36% overall yield from **3**. The H_2O_2 probe **Eu19** was prepared in three steps from **16** and **6*t*-Bu**. HATU mediated coupling of these compounds was followed by acidic *t*-butyl ester cleavage and Eu complexation to give **Eu19** in 48% over these three steps.

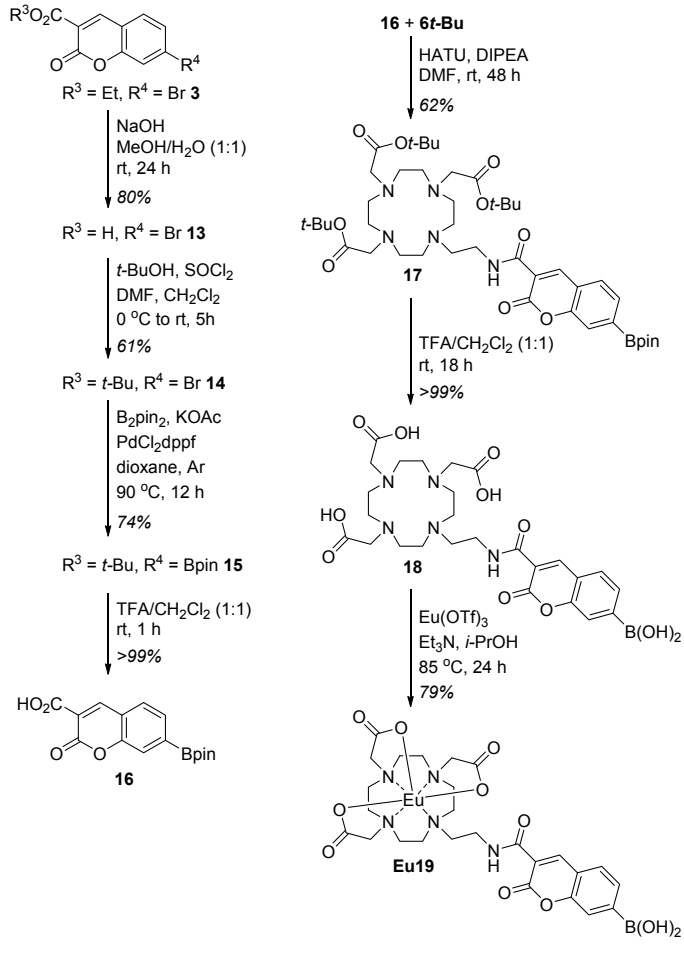

*Scheme 8. Synthesis of **16** and **Eu19**.*

2.2 Probe characterization

The excited state lifetimes (τ), absorption coefficients (ε) and quantum yields (Φ_L) of the probes are summarized in Table 1. Antenna excitation resulted in Eu-centered emission in all cases. The lifetimes in H_2O and D_2O were measured to determine the number of coordinating water molecules (q). The quantum yields were measured using the optically dilute method with

Coumarin 2 (Φ_L = 0.97) as a reference.[67] The overall Eu quantum yield increased about 6-fold when going from the caged **Eu12** to **Eu9**.

Table 1. Photophysical properties of the synthesized probes.

Entry	λ_{max} (nm)	ε (M^{-1} cm^{-1})	Φ_L (%)	τ_{H_2O} (ms)	τ_{D_2O} (ms)	q
Eu9	355	11 000	2.7	0.66	0.66	−0.2
Eu12a	334	9 500	0.39	1.11	2.61	0.2
Eu12b	338	8 700	0.45	1.16	2.50	0.2
Eu19	346	6 900	n.d.	1.15	3.49	0.3

To test the effect of uncaging, it can be informative to analyze the response of the OH analogue to changes in pH, as this can be seen as the simplest form of uncaging. pH titration of **Eu9** revealed that the absorption maximum was shifted upon increasing pH (Figure 10a). At pH < 7 the absorption is centered around 356 nm. Upon increasing the pH this absorption peak disappeared and a new peak corresponding to the phenolate, centered at ~405 nm appeared. This pH dependence was mirrored in the excitation spectrum (Figure 10b). On increasing the pH the Eu emission decreased when exciting at 356 nm and increased when excited at 405 nm. Based on these titrations the pK_a of the phenol was determined to be 6.8. The pH dependence of the probe can be attractive in certain situations. For instance it could potentially enable the selective turn-on of the probe in certain organelles, as the pH within the cell spans from 5−8.[68]

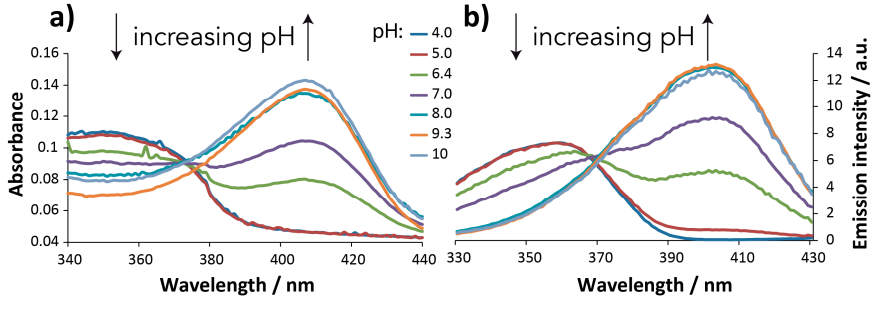

*Figure 10. pH dependence of a) absorption and b) excitation of **Eu9** [**Eu9** (10 µM), HEPES (10 mM), b) λ_{em} = 615 nm].*

Treating **2a** and **4** with H_2O_2 resulted in a similar change, a decreased absorption at ~356 nm and an increase at 405 nm. Coupled to Eu emission this translates to a H_2O_2 dependent decrease in Eu emission when exciting at ~356 nm and an increase when exciting at 405 nm (Figure 11). Such a simultaneous decrease and increase in Eu emission depending on excitation wavelength permits a ratiometric readout which is independent of probe concen-

tration and fluctuations in excitation power.[69] The ratio between the Eu emission when exciting these different absorption bands can thus be used to obtain a more robust readout than simple changes in emission intensity. Plotting this ratio vs [H_2O_2] gave a linear response in the 0−500 µM H_2O_2 range with a ~3-fold contrast window (Figure 11, inset).

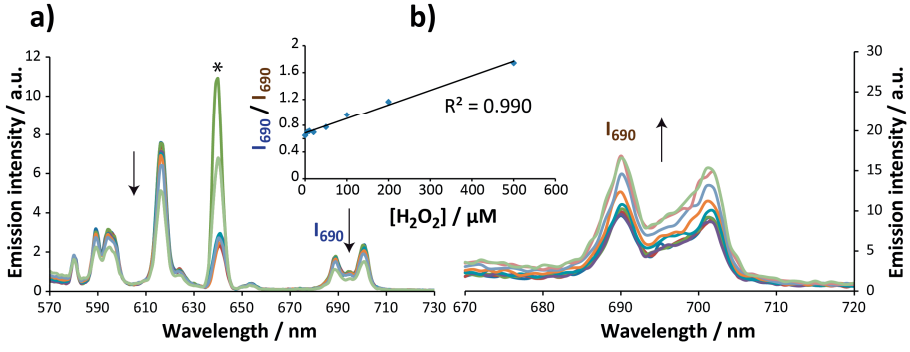

*Figure 11. Changes in the Eu-sensitized emission of **Eu19** in the presence of increasing concentrations of H_2O_2 when exciting at a) 320 nm and b) 400 nm. Inset shows the ratio between the 690 and 690 peak when exciting at 400 and 320 nm, respectively. a) λ_{ex} = 320 nm, b) λ_{ex} = 400 nm, 10 µM **Eu19** in 10 mM phosphate buffer pH 7.5, rt, [H_2O_2]: 0, 5, 10, 20, 50, 100, 200, 500 µM, 45 min incubation time. Arrows indicate the direction of change with increasing [H_2O_2]. The peak marked with asterisk is due to scattered light.*

We next determined the selectivity of the probes to various RONS. The boronate is a well-established H_2O_2-cleavable cage, and has been shown to be selective for this ROS over a wide variety of competing RONS.[58f,64b,d-j] We were expecting to see similar selectivity for our probes. Surprisingly, however, the boronate caged **Eu12a** and **Eu19** probes were not selective towards H_2O_2 but treatment with either $ONOO^-$ or NO resulted in turn-off of Eu emission when the probes were excited at 356 nm (Figure 12). Furthermore, this was coupled to an increased emission when exciting at 405 nm, indicating that these species selectively cleave the caging group rather than unselectively destroy the probe. Interestingly the reaction of $ONOO^-$ with the probes was extremely rapid (76% and 94% decrease of Eu emission after 10 min at pH 7.5 for **Eu19** and **Eu12a**, respectively). $ONOO^-$ is a RNS which is often omitted from similar selectivity studies.

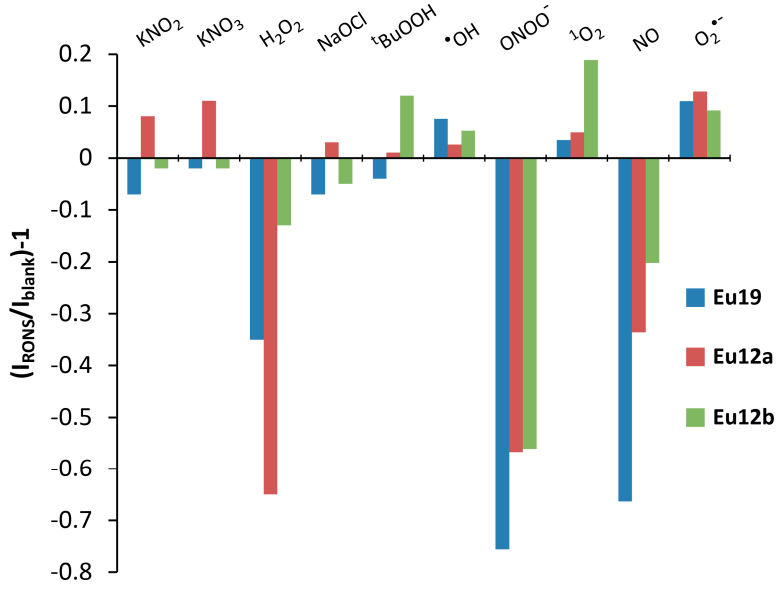

Figure 12. Reaction of Eu complexes with various RONS. Eu complex (10 µM), RONS (200 µM) in HEPES buffer (10 mM, pH 7.5, containing 0.1 mg/mL catalase[70]), λ_{ex} = 356, λ_{em} = 615 nm, time resolved 50 µs delay, 1050 µs sample window). $^{\bullet}OH$ was generated in the Fenton system from $FeSO_4$ and H_2O_2. A stock solution of $ONOO^-$ was generated by mixing aqueous solutions of H_2O_2 (0.65 M) and KNO_2 (0.6 M), the resulting solution was treated with MnO_2 to eliminate excess H_2O_2. The concentration of $ONOO^-$ was determined by measuring its absorption at 302 nm (ε = 1670 M^{-1} cm^{-1}).[71] Singlet oxygen was prepared by mixing equimolar amounts of H_2O_2 and NaOCl in water. NO was generated from diethylenetriamine/nitric oxide adduct. The superoxide solution was generated from a mixture of xanthine (0.1 M) and xanthine oxidase (0.1 unit/mL).

The Eu emission from the *p*-methoxybenzyl caged **Eu12b** was also quenched by $ONOO^-$, and to some extent by NO, but not by H_2O_2. The slow reaction with $O_2^{\bullet-}$ seen for **2b** in DMSO (see above) was not seen for **Eu12b**, presumably due to rapid dismutation of $O_2^{\bullet-}$ in H_2O. The $ONOO^-$ quenching of **Eu12b** was concentration dependent and persisted long after the lifetime of $ONOO^-$, suggesting that the change is due to a reaction between **Eu12b** and $ONOO^-$. However, we were not able to determine the identity of the reaction product.

To further investigate the uncaging reaction of these RONS we determined the pseudo-first order rate constants of **2a** and **4** with H_2O_2 and $ONOO^-$ (Table 2). The rate constants for the reactions of **2a** and **4** with excess H_2O_2 was measured by following the changes in coumarin absorption at 405 nm for the first 20 min at 5 different H_2O_2 concentrations, and plotting the initial rates vs [H_2O_2]. The reaction with $ONOO^-$ was measured using a stopped-flow instrument.[72] In these experiments the coumarin emission was monitored, as nitrite (which is formed in the reduction of $ONOO^-$) absorbs at

354 nm, which interfered with coumarin absorption measurements. It was necessary to use $ONOO^-$ as the limiting reagent as high $ONOO^-$ concentrations led to degradation of the coumarins.

Table 2. Rate constants ($M^{-1} s^{-1}$) for the reaction of **2a** and **4** with H_2O_2 and $ONOO^-$.

RONS	**2a**	**4**
H_2O_2	0.900	0.173
$ONOO^-$	3.00×10^3	1.68×10^5

Benzyl caged **2a** reacted 5.2-fold faster than **4** with H_2O_2. These results agree with those reported by the Cohen group who noted similar differences between benzyl-linked boronates and aryl boronates.[66] Interestingly **4** reacts one million times faster with $ONOO^-$ than with H_2O_2. These values are in line with those reported by Kalyanaraman and coworkers.[73] The rate constant for quinone methide elimination has been determined to be 540 $M^{-1} s^{-1}$ for a similar system.[74] This means the rate determining step for the full uncaging of **2a** with H_2O_2 is the boronate oxidation, whereas in the reaction of **2a** with $ONOO^-$ it is the quinone methide elimination.

2.3 Conclusion

Eu complexes equipped with long-wavelength absorbing coumarin antennae have been prepared. The feasibility of rendering these complexes analyte responsive was demonstrated by introducing RONS cleavable caging groups in the coumarin 7-O-position. H_2O_2 has both beneficial and harmful roles in the cell. It acts as a second messenger mediating cell signaling by redox based mechanisms but its overproduction in mitochondria has been implicated in the development of various diseases. $ONOO^-$ is involved in inflammation.[71] Reliable detection of these species is of great value. This design, however, is not limited to the analytes reported here but could easily be extended to others by incorporating different caging groups.[75]

3. Luminescent lanthanide complexes with analyte triggered antenna formation (paper II)

Caging of phenol and aniline derivatives with chemoselectively cleavable caging groups is a commonly utilized and powerful strategy for rendering luminophores analyte responsive.[53] However, one drawback of such an approach is the pH sensitivity of the turned-on probe, as the protonated species often has photophysical properties similar to that of the caged compound (see above). A popular strategy to minimize this problem is to make the phenol or aniline less prone to protonation by incorporating electron withdrawing groups into the fluorophore. Such an approach has successfully been applied to fluorescein[76] and coumarin[30d] derivatives. Another, less widely used approach is to design the probe so as to make the uncaging part of a tandem process which masks the formed phenol or aniline.[27,75c,d]

The coumarin structure comprises of two joined aromatic systems, one of which incorporates a lactone (Scheme 9a). Caging of the lactone oxygen has been shown to be a viable strategy for placing coumarin emission under analyte control. Initial uncaging and phenolate formation leads to subsequent lactonization and coumarin formation (Scheme 9b). Coumarin formation results in a rigidification of the molecule which should lessen vibrational deactivation of the excited state and hence increase the quantum yield. We hypothesized that when coupled to a Ln the coumarin formation would result in an increase of the sensitized Ln emission. Caged coumarin precursors have been used to detect F^-[75c] and Hg^{II}.[75d] However, having Ln-emission as a readout would provide the benefits of narrow, long-lived Ln-emission. In addition, if several Lns with different emission colors can be sensitized a palette of Ln probes can be created from the same core structure.

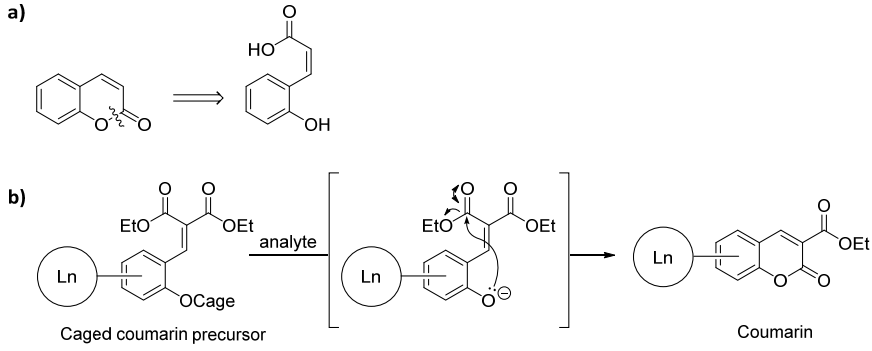

Scheme 9. a) Coumarin structure. b) Idea behind the analyte-triggered coumarin formation.

To explore the feasibility of this approach, we decided to construct caged coumarin precursors with cages for a wide variety of analytes. We settled for Pd^0 (using an allyl cage[77]), H_2O_2/$ONOO^-$ (boronate cage[78]), β-galactosidase (β-galactose cage[75b]) and F^- (TIPS cage[75c]). While H_2O_2 and β-galactosidase have biological relevance (see above), Pd and F^- are environmental contaminants in roadside dust and drinking water, respectively.

The general design of these 2nd generation probes is shown in Scheme 10 (**Ln22**). We were concerned that the harsh reaction conditions employed during the Ln complex synthesis (strong acids and prolonged heating with Ln salts) might limit the scope of caging groups employable. For this reason we chose a convergent synthesis where the coumarin precursors and Ln complexes are coupled in the final step under Cu-catalyzed azide-alkyne cycloaddition (CuAAC) conditions (Scheme 10).[79] As the Ln, we chose Eu and Tb (red and green emitting, respectively), for which coumarins are well known sensitizers,[80] as well as Sm (orange emitting).

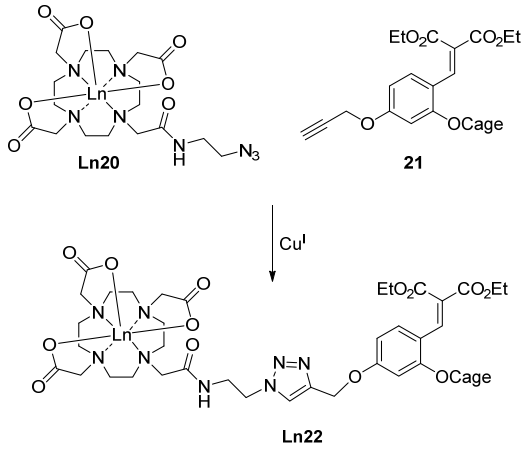

Scheme 10. Coupling approach to access Ln-based probes.

3.1 Synthesis

The Ln complexes **Ln20** were synthesized in four steps from cyclen (**23**) (Scheme 11). Monoalkylation of cyclen with azide **24**[81] in $CHCl_3$ at room temperature gave **25** in 82% yield. Trialkylation with *t*-butyl bromoacetate, followed by subsequent cleavage of the *t*-butyl esters in TFA/CH_2Cl_2 (1:1) provided the ligand **27** in 85% yield over these two steps. Finally the Eu, Sm, and Tb complexes **Ln20** were prepared in good yields from **27** by reacting it with the corresponding chloride (for Eu and Tb) or triflate salts (for Sm) in a MeOH/H_2O mixture adjusted to pH 8.

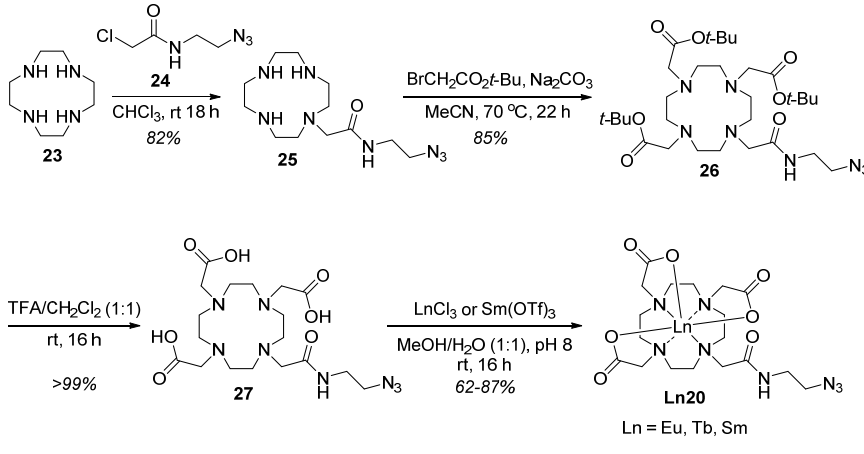

*Scheme 11. Synthesis of Ln complexes **Ln20**.*

We next focused on the caged coumarin precursors. Our initial strategy was to introduce the boronate cage directly into **28**. However, this proved problematic, likely due to cleavage of the palladium sensitive O-propargyl group under the borylation conditions (Scheme 12).

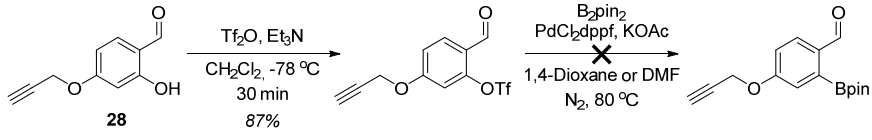

*Scheme 12. Attempted borylation of **28**.*

To circumvent this problem the boronate was instead attached *via* a self-immolative *p*-benzyl linker. The boronate cage **31** was synthesized starting from *p*-bromotoluene (**29**) (Scheme 13). Miyaura borylation in dioxane gave the boronate ester **30** in good yield.[82] Bromination of the benzylic position was achieved using NBS and AIBN as initiator. In addition to **31**, minor amounts of the dibrominated analogue were also formed in this reaction. The β-galactosidase cage **34** was synthesized in a related fashion (Scheme 13). Glycosylation of *p*-cresol using the trichloroacetimidate donor **32** was followed by radical bromination. Again, bromination resulted in minor amounts of dibrominated product. Due to the almost identical polarities of the mono- and dibrominated products these could not be separated, and **31** and **34** were used in the subsequent steps with this minor impurity.

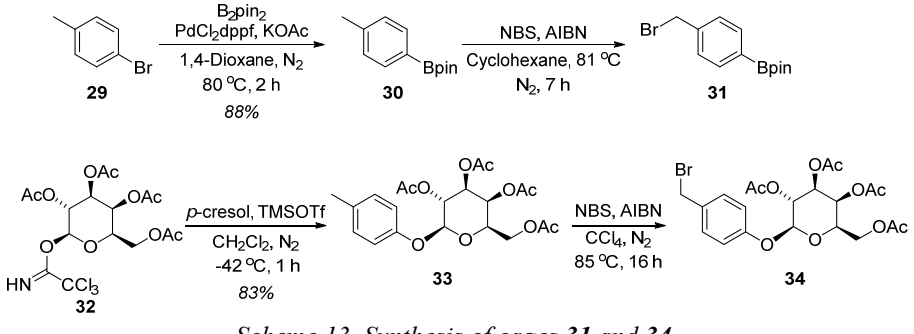

*Scheme 13. Synthesis of cages **31** and **34**.*

Next, the caged coumarin precursors were synthesized (Scheme 14). Salicylaldehyde **28** was O-alkylated with the bromides **e-g** or silylated with TIPS-Cl (**h**). This was followed by Knövenagel condensation with diethyl malonate to yield the caged antennae **21e**,**f**,**h**. For the β-galactose caged coumarin, Knövenagel condensation was followed by a deacetylation step in basic methanol to give the methyl ester **21g**.

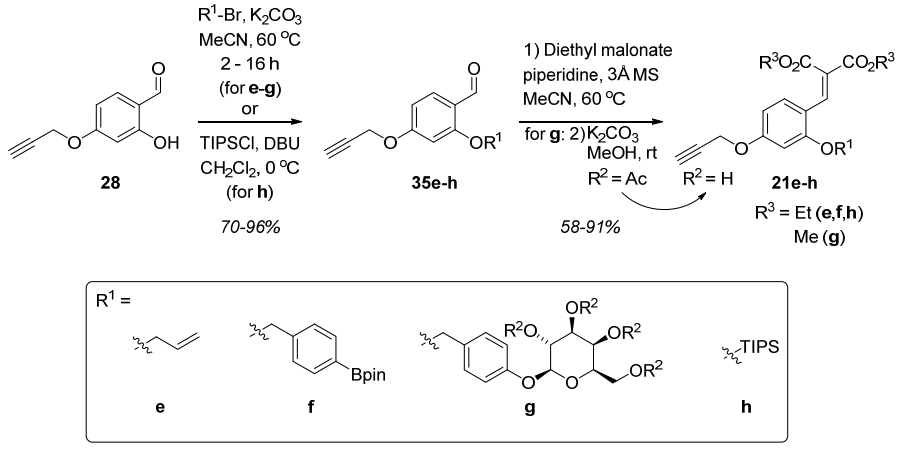

*Scheme 14. Synthesis of the caged coumarin precursors **22e-h**.*

Finally, the caged precursors **21e-h** were coupled with the Ln complexes **Ln20** under copper-catalyzed conditions (Scheme 15).[79] This reaction turned out to be unexpectedly sluggish, and required some experimentation in order to proceed at any detectable rate. The poor performance of this reaction led us to investigate how it could be improved for Ln complex synthesis (Chapter 5).

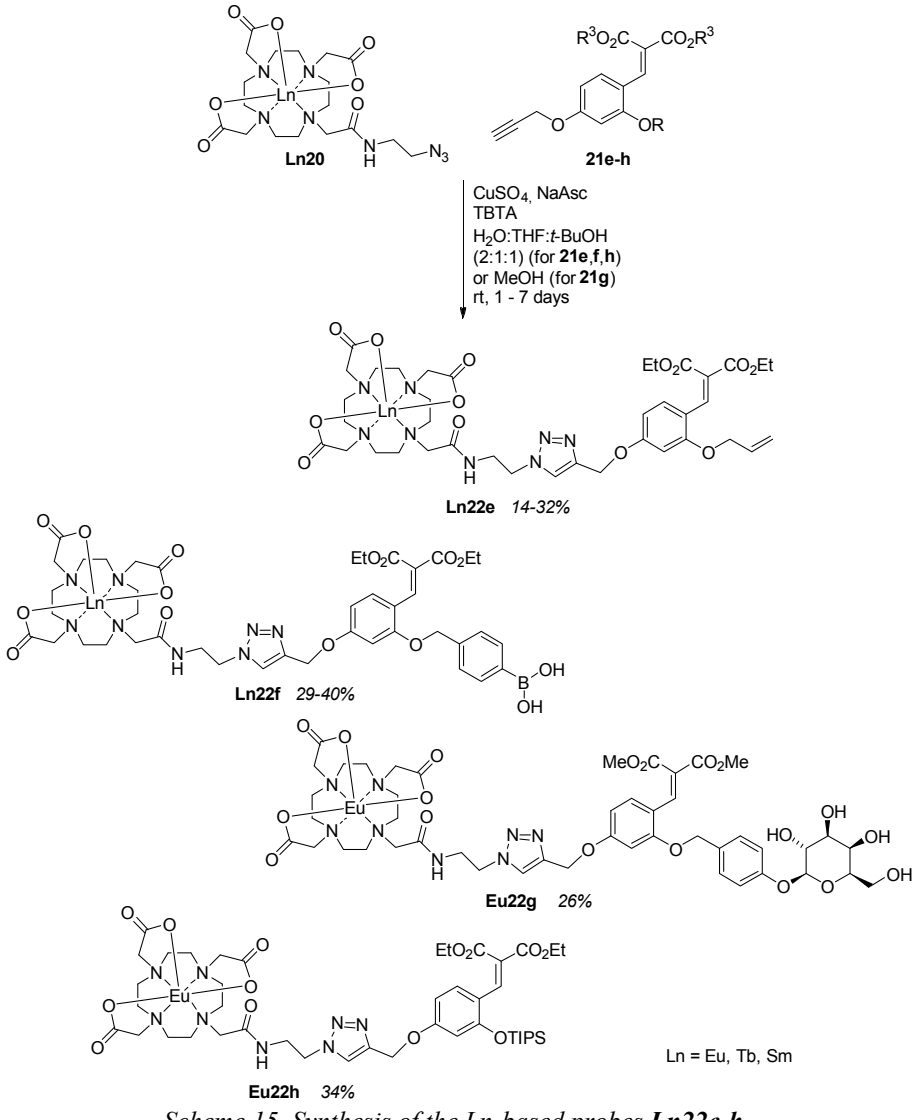

*Scheme 15. Synthesis of the Ln-based probes **Ln22e-h**.*

In addition to these analyte-responsive complexes, the corresponding coumarin compounds were also synthesized as references (Scheme 16).

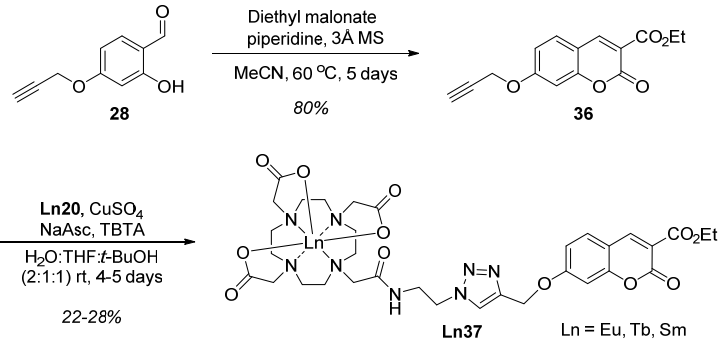

*Scheme 16. Synthesis of **Ln37**.*

The final Ln-based probes could be obtained as hygroscopic solids in 14−40% yield after purification by column chromatography and subsequent freeze drying.

3.2 Probe characterization

In order to assess whether analyte-triggered coumarin formation occurred as expected we first monitored the reactions of **21e**,**f,h** → **36** by ^{1}H-NMR spectroscopy. Treatment of these compounds with their respective analytes resulted in a decrease in the ^{1}H-NMR peaks arising from the caging group. Coupled coumarin formation was seen for **21e** and **21h**.[83] However, in the case of **21f** conversion to the coumarin was considerably slower and was not observed in the ^{1}H-NMR spectrum after 1 h, but could be confirmed by mass spectrometry. We attribute this difference in coumarin formation rates to the different solvents used (MeOD-d_4 for **21f** vs. DMSO-d_6 for **21e**,**h**). Changing the solvent can affect the rate by several orders of magnitude[84] and the presence of additives (e.g. F^-) can also be significant.[75c] Supporting evidence of analyte triggered coumarin formation from **21e**,**f,h** was found from fluorescence spectroscopy which showed the emergence of a broad peak centered at ~405 nm, characteristic of coumarin emission.

Fluorescence spectroscopy revealed that the caged probes **Ln22** (λ_{max} = 335 nm) were essentially nonemissive when excited at 356 nm. In comparison, irradiation of the corresponding coumarin complexes **Eu37** and **Tb37** (λ_{max} = 356 nm) at this wavelength generated intense Ln-centered emission. **Sm37** was also emissive but its brightness was much lower than that of **Eu37** and **Tb37**. For this reason, we focused on the Eu- and Tb-based probes. The luminescent lifetimes of **Eu37** and **Tb37** in H_2O and D_2O were determined, and based on these values the hydration states q were calculated (Table 3).[41] The calculated q ~1 for **Eu37** is in line with the eight-coordinate DO3A ligand structure.[54c] However the unexpectedly large value

for **Tb37** (q ~3) is indicative of energy back transfer from Tb to the antenna. We could also see that the emission intensity of **Tb37** increased in the absence of oxygen, which lends further support to the energy back transfer hypothesis.

Table 3. Photophysical properties of **Eu37** and **Tb37**

Compound	τ_{H_2O} (ms)	τ_{D_2O} (ms)	q	Φ_L (%)
Eu37	0.71	2.73	0.87	0.31
Tb37	0.46	0.64	2.72	n.d.

The emission intensity of **Eu37** as a function of pH was also assessed and as expected, it was essentially unchanged in the pH range 4−8. When we treated the probes **Ln22e-h** with their respective analytes intense turn-on of the sensitized Ln emission was observed.

3.2.1 Palladium probe **Eu22e**

Luminescence titration of **Eu22e** with $Pd(PPh_3)_4$ revealed a linear response in the 0−8 μM range with a 40-fold emission turn-on (8 μM [Pd^0], 10 min) (Figure 13). **Eu22e** could detect [Pd^0] as low as 80 nM. In the presence of a reducing agent such as PPh_3, Pd^{II} could also be detected indirectly.

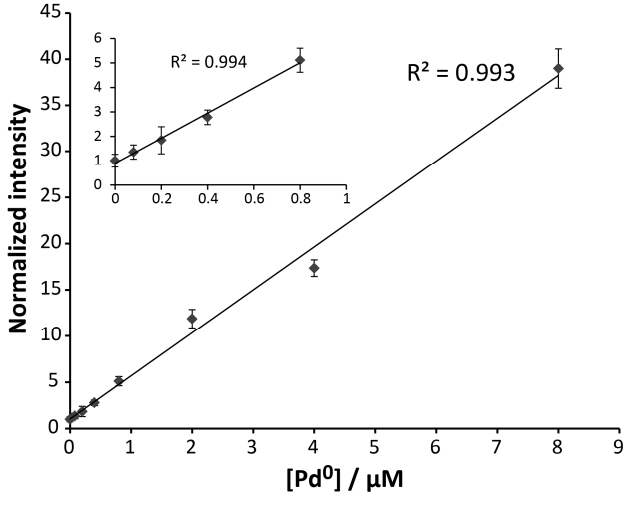

*Figure 13. Luminescence titration of **Eu22e** with $Pd(PPh_3)_4$ [10 μM **Eu22e**, MeCN: borate buffer pH 10 (1:1), 10 min, rt, steady state, λ_{ex} = 356 nm, λ_{em} = 699 nm. Error bars show standard error based on three independent experiments. Intensities are normalized to that of the blank].*

The selectivity for Pd^0 versus various metal cations was also determined (Figure 14). Of the metals tested only Pt^{II} resulted in increased emission

(18% compared to Pd^0). Competition experiments revealed that Pd^0 could be detected in the presence of all these cations except Au^{III}. This may be due to oxidation of Pd^0 by Au^{III} (1.401 eV for the Au^{III}/Au^{I} pair vs 0.951 eV for Pd^{II}/Pd^0).[85]

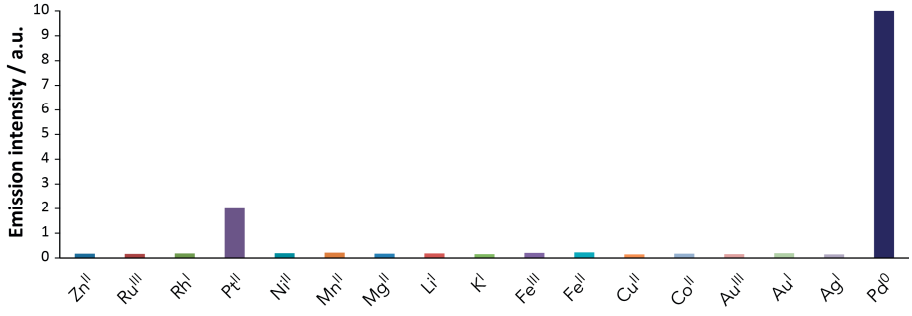

*Figure 14. Luminescence response of **Eu22e** to various metal cations [**Eu22e** (20 µM), 50 µM metal cation, MeCN:borate buffer pH 10 (1:1), 10 min, rt, λ_{ex} = 356 nm, λ_{em} = 615 nm, time resolved, 50 µs delay, 1050 µs sample window].*

3.2.2 H_2O_2 probe **Eu22f**

The emission of **Eu22f** responded linearly to increasing H_2O_2 concentrations (Figure 15). H_2O_2 could be detected down to 1 µM. In the presence of a large excess of H_2O_2 (1 mM, 30 min) a 30-fold turn-on response was observed. In addition to H_2O_2 this probe is expected to respond to $ONOO^-$, however this was not investigated at the time.

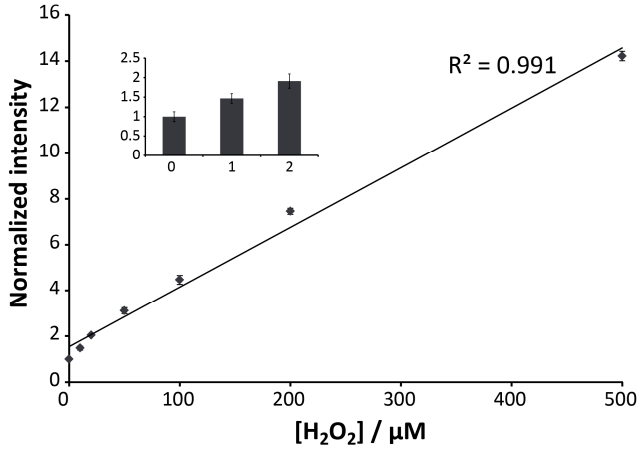

*Figure 15. Luminescence titration of **Eu22f** with H_2O_2 [**Eu22f** (10 µM), pH 7 HEPES buffer, 1 h, rt, λ_{ex} = 356 nm, λ_{em} = 615 nm, time-resolved, 50 µs delay, 1050 µs sample window). Inset: normalized Eu luminescence at [H_2O_2] = 0, 1, and 2 µM (1.5 h, rt, λ_{em} = 594 nm). Error bars show standard error based on three independent experiments. Intensities are normalized to that of the blank].*

3.2.3 Fluoride probe **Eu22h**

Treatment of **Eu22h** with TBAF gave a concentration dependent emission increase in the 0−100 µM range. However, compared to the other probes, the response was modest with only a ~2 fold increase in Eu emission (Figure 16).

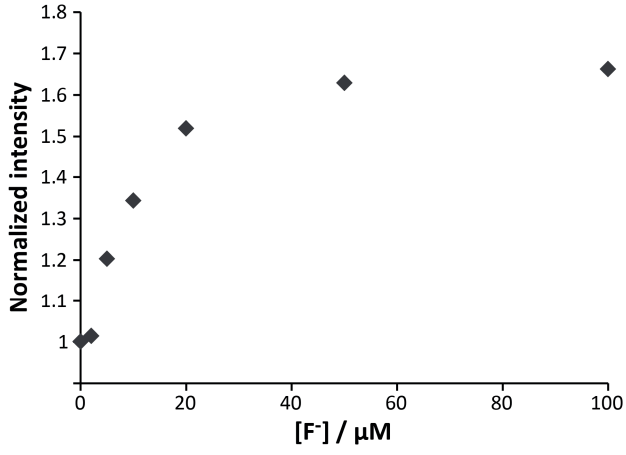

*Figure 16. Emission intensity of **Eu22h** upon treatment with increasing concentrations of TBAF [**Eu22h** (10 µM) in DMSO, steady state, λ_{ex} = 356 nm, λ_{em} = 618 nm. Intensities are normalized to that of the blank].*

3.2.4 β-Galactosidase probe **Eu22g**

Treatment of a 1 µM solution of **Eu22g** with one unit of β-galactosidase yielded an intense emission turn-on (~16-fold after 10 min in phosphate buffer, pH 7.0). A similar response was observed in cell lysate of bacteria expressing β-galactosidase (Figure 17).

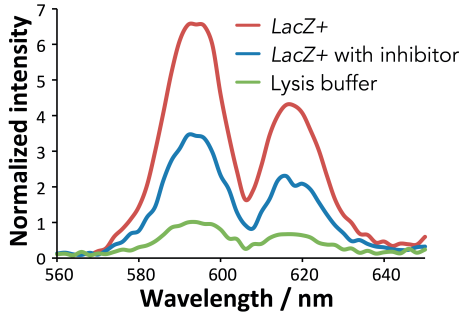

*Figure 17. Emission of **Eu22g** in cell lysate [**Eu22g** (25 µM), 5 min, 25 °C, λ_{ex} = 356 nm, time resolved, 50 µs delay, 1050 µs sample window. Intensities are normalized to that of the blank].*

To our delight, **Eu22g** could also be used to detect β-galactosidase in live *LacZ*+ bacteria. Both **Eu22g** and **Eu37** appeared non-toxic to these cells as they did not interfere with bacterial growth (in the 0−25 μM [**Eu22g**] and [**Eu37**] range). We also established that the uptake and turnover of **Eu22g** was less than 10 min. When we incubated **Eu22g** with live *LacZ*+ bacteria a time-dependent emission increase was observed (Figure 18). In contrast, no increase of emission was observed with **Eu22g** in the presence of *LacZ*− bacteria.

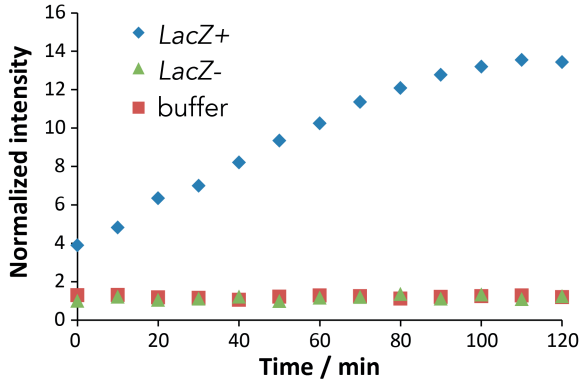

*Figure 18. Monitoring of real time β-galactosidase activity in live bacteria with **Eu22g** [**Eu22g** (10 μM), λ_{ex} = 356 nm, λ_{em} = 590 nm, 37 °C, time resolved, 50 μs delay, 1050 μs sample window. Intensities are normalized to that of the first data point of the blank].*

3.3 Conclusion

A novel design strategy for constructing Ln-based responsive probes has been developed. The design enables access to Eu- and Tb-based probes for a wide variety of chemically distinct species. Because the coumarin formation relies on the unmasking of a phenolic OH, in principle any species which mediates this reaction can be detected with this design. The feasibility of this approach was demonstrated by preparing Ln-based probes for four different analytes (Pd^0, H_2O_2, F^- and β-galactosidase), some of which have properties comparable to those of the best organic-based probes for these species (**Eu22e**[75a,77] and **Eu22f**[64d,e]) and are superior to previously reported Ln-based probes (**Eu22f**[58a,86]).

4. Multiplex detection with responsive lanthanide-based luminescent probes (papers II & III)

Studying multiple processes in complex systems such as live cells simultaneously and non-invasively is a challenging project. Fluorescence spectroscopy is very well suited for this task due to its high spatial and temporal resolution. However, using multiple organic fluorophores can be difficult due to their broad emission bands which can lead to spectral cross-talk (see above). The lanthanides provide a clear advantage in this respect with their narrow, non-overlapping emission signals. Although non-responsive Ln complexes are well established for multicolor labeling,[52] multiplex analyte detection using responsive Ln complexes has never been achieved.

We were interested in exploring the possibility of multi-analyte detection using our probes. The ability of the 2nd generation probes to sensitize both Eu and Tb together with the fact that these Lns have non-overlapping emission signals should make this possible. The emission spectra of Eu and Tb are shown in Figure 19. The most intense non-overlapping bands are the Tb $^5D_4 \rightarrow {}^7F_5$ (545 nm) and Eu $^5D_0 \rightarrow {}^7F_5$ (705 nm). However, detection of the Eu $^5D_0 \rightarrow {}^7F_5$ emission was impossible with our experimental setup due to interference at this wavelength from scattered excitation light (luminescence plate reader with 350 nm excitation). Hence for the multicolor detection we monitored the Tb $^5D_4 \rightarrow {}^7F_5$ (545 nm) and Eu $^5D_0 \rightarrow {}^7F_3$ (655 nm) bands. It should be noted, however, that monitoring of the Eu $^5D_0 \rightarrow {}^7F_5$ emission is possible on a spectrofluorometer.

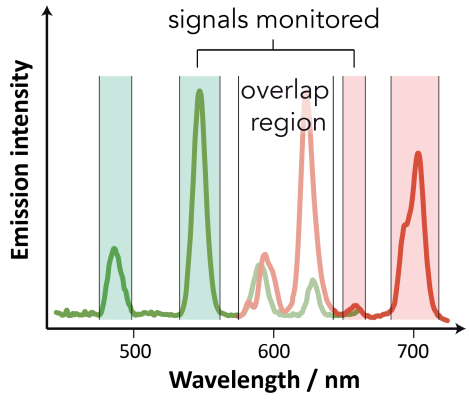

Figure 19. Illustration of Tb (green) and Eu (red) emissions monitored in the two analyte detection experiments.

To test the possibility of multicolor detection we initially subjected a mixture of the H_2O_2 probe **Tb22f** and the F^- probe **Eu22h** to H_2O_2 and TBAF (Figure 20). Adding only H_2O_2 or TBAF resulted in an increase only in the Tb or Eu emission, respectively. Adding both H_2O_2 and TBAF gave an increase in both the Tb and Eu emissions. The slight decrease in Eu emission with H_2O_2 and F^- compared to only F^- is presumably due to competing absorption of the produced **Tb37**.

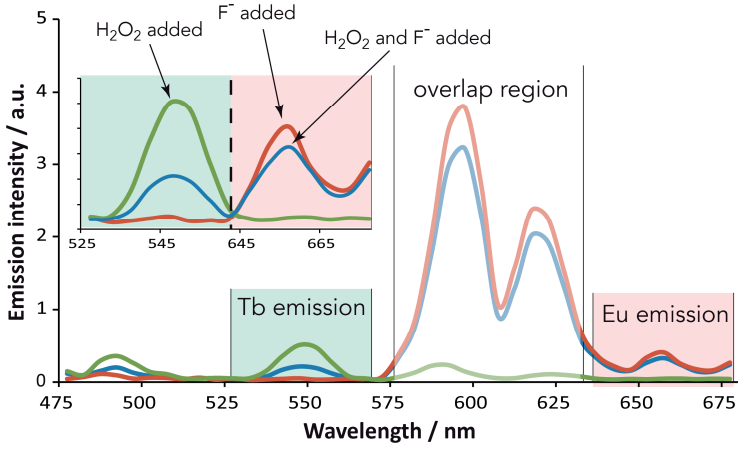

*Figure 20. Detection of H_2O_2 and F^- simultaneously. Blue: 200 µM F^-, 50 µM H_2O_2; red: 200 µM F^-; green: 200 µM H_2O_2. [**Tb22f** and **Eu22h** (10 µM), pH 7.0 HEPES buffer (10 mM), 1 h, time-resolved, 50 µs delay, 1050 µs sample window].*

While the simultaneous detection of H_2O_2 and F^- shows the possibility of multicolor imaging with our probes, it is of little practical use. In light of this we were interested in applying our probes for the detection of more challenging and, potentially, useful analyte combinations. Monitoring multiple

enzymatic activities in real time is one such application, with potential uses in drug development, disease diagnostics and biochemical assays. To expand the analyte space in the enzyme domain we decided to synthesize additional coumarin precursors, caged with β-glucose (β-glucosidase), α-mannose (α-mannosidase) and phosphate (phosphatase).

We were particularly excited by the prospect of extending the simultaneous detection to three different analytes. While this could in theory be done with probes based on three different Lns such as Eu, Tb and Sm, or Eu, Tb and Dy, the compound **Sm37** was essentially non-emissive, precluding its use. We were hopeful that by shortening the Ln-antenna distance, the energy transfer efficiency (and hence the brightness) would be sufficiently improved as to allow the use of Sm and Dy. The new design is shown in Scheme 17.

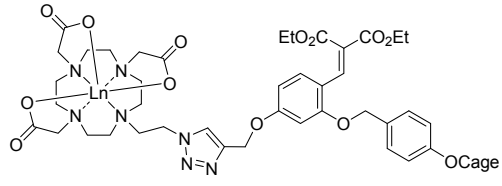

Ln38 Ln = Eu, Tb, Sm, Dy

Scheme 17. General structure of 3rd generation probes.

4.1 Synthesis of 3rd generation probes

The caged coumarin precursors were synthesized as shown in Scheme 19. **34Glu** and **34Man** were synthesized in the same fashion as **34Gal** (Chapter 3, Scheme 13)**,** with glycosylation of *p*-cresol using the corresponding glycosyl trichloroacetimidate donors, followed by radical bromination. The phosphate functionalized **34Phos** was synthesized in three steps by phosphorylation of **39** followed by reduction of the aldehyde and mesylation to give **34Phos** in 72% yield over these three steps (Scheme 18).

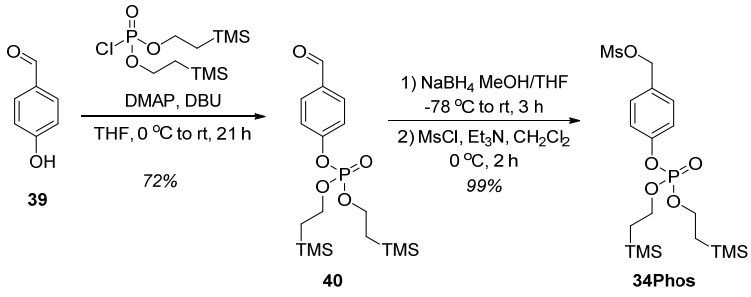

*Scheme 18. Synthesis of **34Phos**.*

The caged coumarin precursors **21** were synthesized from salicylaldehyde derivative **28** in three steps (Scheme 19). Alkylation of salicylaldehyde **28** was followed by condensation with diethyl malonate and deprotection to give the caged coumarin precursors **21**.

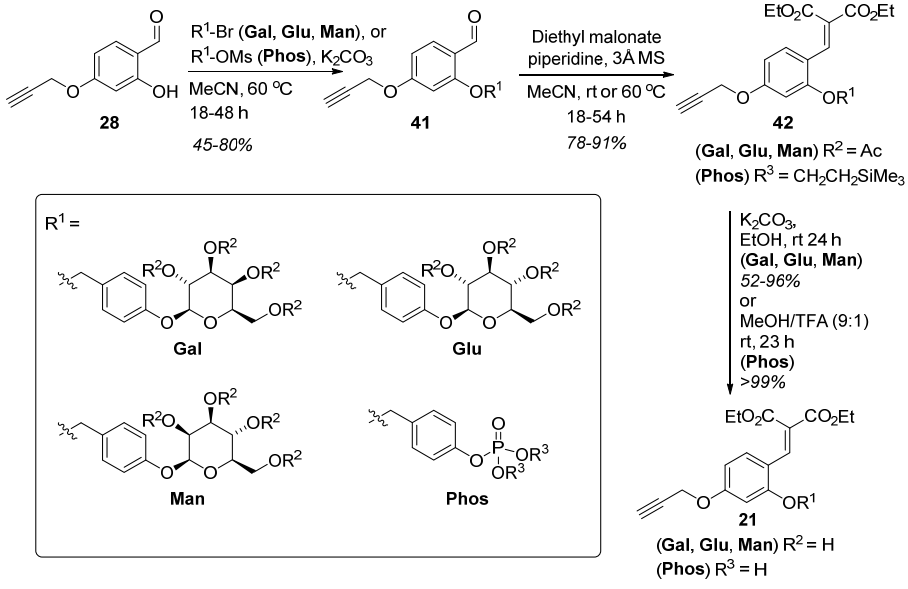

*Scheme 19. Synthesis of the caged coumarin precursors **21**.*

The caged coumarin precursors **21** were then coupled to the DO3A derivative **Ln47** under CuAAC conditions (Scheme 20). The synthesis of **Ln47** as well as optimization of the CuAAC conditions is discussed in Chapter 5. After the reaction the compounds were isolated by removal of the DMSO with repeated precipitation of the product in MeOH/Et_2O, and subsequent purification by silica column chromatography using MeCN/H_2O as eluent.

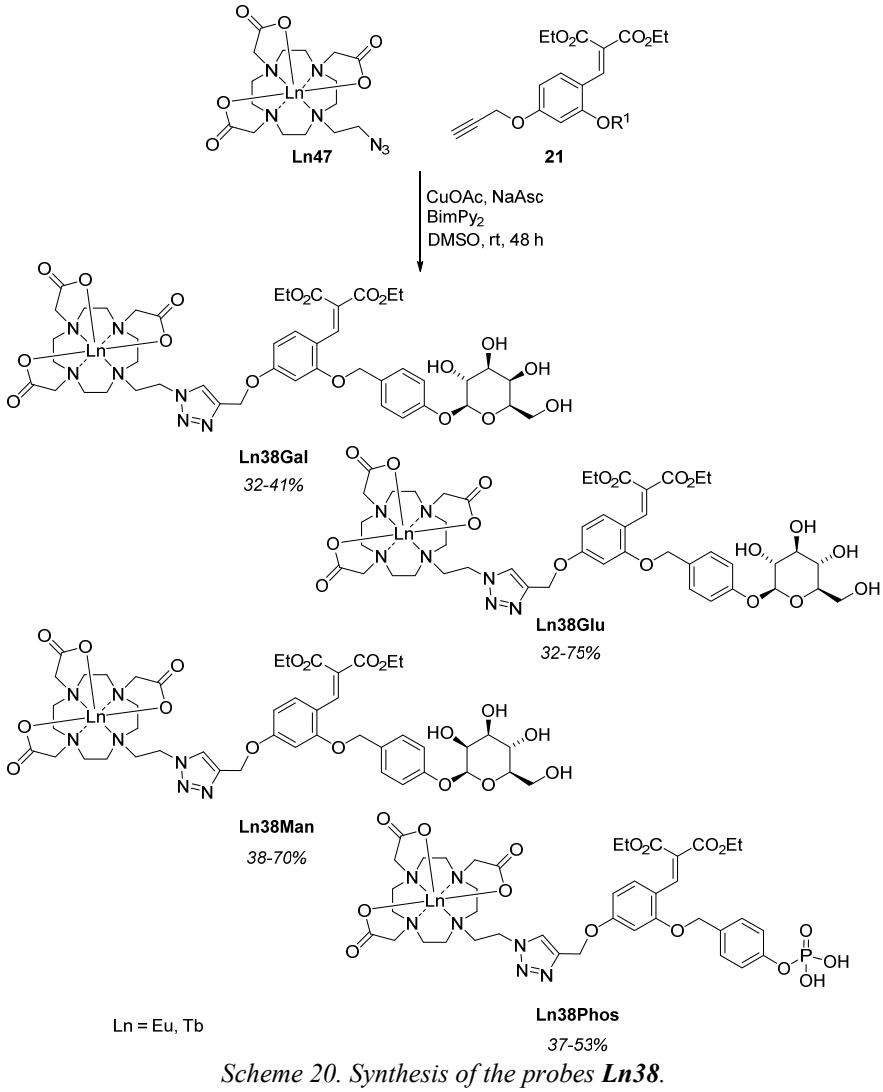

*Scheme 20. Synthesis of the probes **Ln38**.*

In addition to these probes the reference compounds **Ln38Bn** and **Ln43** were synthesized (Scheme 21).

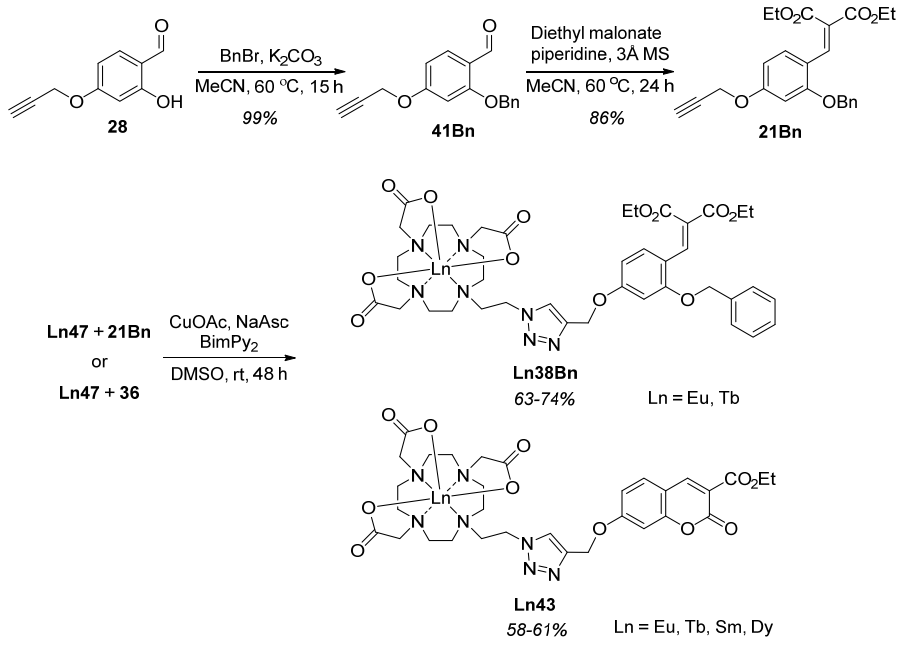

*Scheme 21. Synthesis of reference compounds **Ln38Bn** and **Ln43**.*

4.2 Probe characterization

All Eu and Tb compounds gave Ln-centered emission when excited through the chromophore. These 3rd generation probes were somewhat brighter than the 2nd generation complexes (3.5-fold increase in Φ_L of **Eu43** compared to **Eu37**), presumably resulting from a more efficient sensitization due to the shorter antenna-Ln distance. Unfortunately, **Sm43** and **Dy43** were non-emissive despite the shorter linker. The photophysical properties of the reference compounds are summarized in Table 4. The negative q value of **Tb38Bn** could be due to multiple deactivation pathways of the Tb excited state.

Table 4. Photophysical characterization of the reference compounds.

Entry	λ_{max} (nm)	ε ($M^{-1}cm^{-1}$)	Φ_L (%)[a]	τ_{H_2O}	τ_{D_2O}	q
Eu38Bn	335	7600	0.12 (0.9)	1.17	3.38	0.37
Tb38Bn	335	4500	0.41 (0.7)	0.97	0.69	−2.41
Eu43	350	13200	1.08 (37)	1.23	3.50	0.33
Tb43	350	13000	1.63 (32)	0.72	0.77	0.15

[a]Φ_L in parenthesis refers to the antenna fluorescence quantum yield.

Comparison of the emission spectra of the caged references and those of the coumarin-equipped complexes revealed the upper limit of turn-on for these probes to be 54-fold and 10-fold for the **Eu43**/**Eu38Bn** and **Tb43**/**Tb38Bn** combinations, respectively (Figure 21).

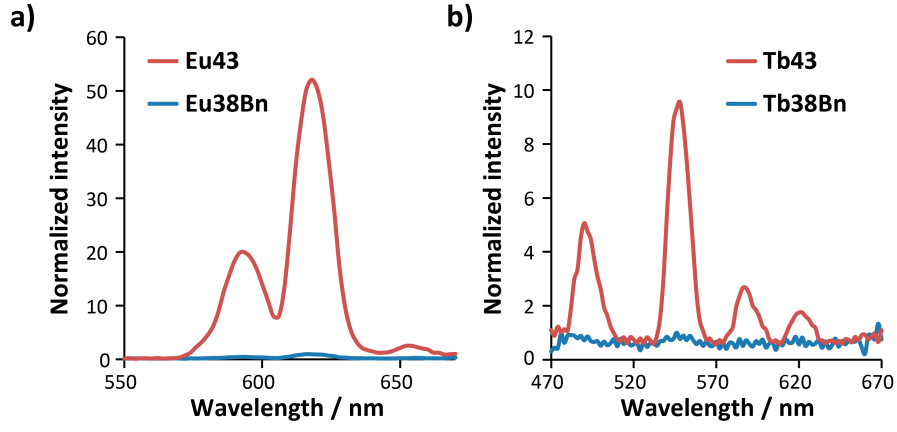

*Figure 21. Comparison of the Ln-sensitized emission of the caged reference compounds **Ln38Bn** to the coumarin complexes **Ln43** (25 µM in 100 mM HEPES pH 7.0, 25 °C, λ_{ex} = 356 nm, time resolved, 250 µs delay, 1050 µs sample window. Intensities are normalized to that of the highest intensity signal of **Ln38Bn**).*

Treatment of the various probes with their respective analytes resulted in a robust turn-on of the sensitized Ln-emission (Figure 22). Unfortunately, probe processing seemed to slightly deactivate the enzymes, as determined by plotting the emission intensity vs. [enzyme]×time at different enzyme concentrations (Selwyn's test).[87] For this reason, we were unable to determine the K_m and v_{max} values for the various enzyme-probe combinations.

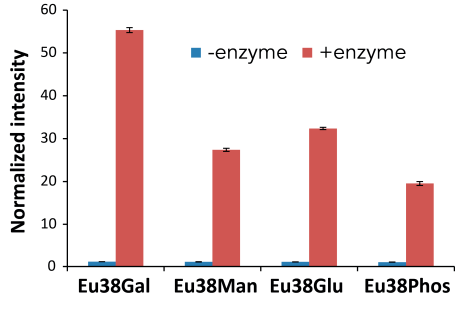

*Figure 22. Turn-on of the Eu-based probes when treated with their respective analytes [**Eu38** (50 µM), β-galactosidase (0.25 U), α-mannosidase (1 U), β-glucosidase (5 U), alkaline phosphatase (0.1 U), 1 h, 25 °C, 100 mM HEPES pH 7.0 or pH 8.0 (**Eu38Phos**), λ_{ex} = 356 nm, λ_{em} = 615 nm, 250 µs delay, 1050 µs sample window. Error bars show standard error based on three independent experiments. Intensities are normalized to that of the blank for each probe].*

4.2.1 Multicolor detection

We next turned our attention to the detection of multiple enzymatic activities simultaneously. The glycosidases turned out to be quite promiscuous which precluded the detection of certain enzyme combinations (Figure 23).

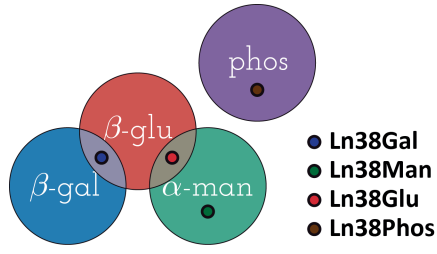

Figure 23. Cross-reactivity observed between the enzymes used.

Subjecting a mixture of **Tb38Gal** and **Eu38Phos** to either β-galactosidase or alkaline phosphatase resulted in an increase in the sensitized Tb and Eu emissions, respectively (Figure 24a, columns 2 and 3). Treating this mixture of probes with both enzymes resulted in an increase in both the Tb and Eu emissions (Figure24a, column 4). β-galactosidase and α-mannosidase were also readily detected simultaneously using an orthogonal combination of **Ln38Gal** and **Ln38Man** (Figure 24b).

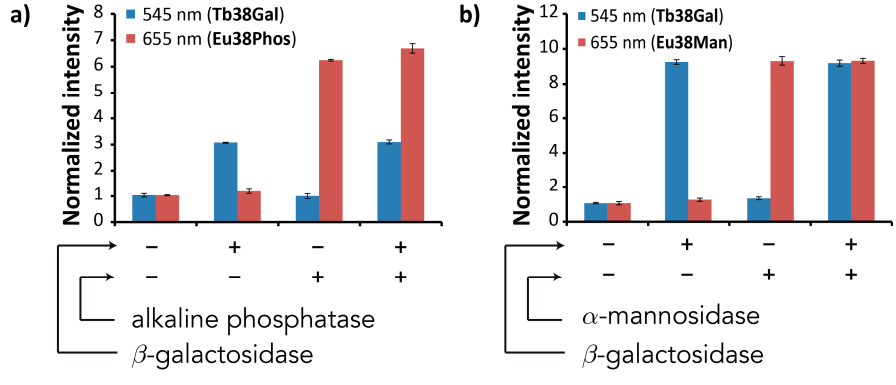

*Figure 24. Multiplex detection of a) β-galactosidase and alkaline phosphatase activity and b) β-galactosidase and α-mannosidase activity. a) **Tb38Gal** (25 µM) **Eu38Phos** (12.5 µM), alkaline phosphatase (0 or 0.1 U), β-galactosidase (0 or 0.5 U), 20 min 25 °C (HEPES 100 mM, NaCl 1 M, $MgCl_2$ 5 mM and $ZnCl_2$ 0.2 mM, pH 8.0); b) **Tb38Gal** and **Eu38Man** (25 µM), α-mannosidase (0 or 0.2 U), β-galactosidase (0 or 0.5 U), 4 h, 25 °C, (100 mM HEPES pH 7.0); λ_{ex} = 356 nm λ_{em} = 545 & 655 nm, time-resolved, 250 µs delay, 1050 µs sample window. Error bars show standard error based on three independent experiments. Intensities are normalized to that of the blank for each probe.*

Finally, we wanted to explore the possibility of detecting three analytes simultaneously. The low brightness of **Sm43** and **Dy43** precluded the use of these Lns in our responsive probes. We instead turned to the organic fluorophore **4** (Chapter 2, Scheme 5). The boronate of **4** can be oxidized by H_2O_2 to form the corresponding 7-OH coumarin, which is excitable at 410 nm and emits at 450 nm (Figure 25). Using this probe together with **Eu38Gal** and **Tb38Phos** it was possible to detect the three non-interacting analytes H_2O_2, β-galactosidase and alkaline phosphatase simultaneously (Figure 26a). Adding only H_2O_2, alkaline phosphatase or β-galactosidase to a mixture of probes **4**, **Tb38Phos** and **Eu38Gal** resulted in an increase in the coumarin, Tb and Eu emissions, respectively (Figure 26a, columns 2−4). Any two-analyte combinations gave the expected luminescence response (Figure 26a, columns 5−7). Finally, adding H_2O_2, β-galactosidase and alkaline phosphatase simultaneously resulted in an increase in all emission intensities. (Figure 26a, column 8).

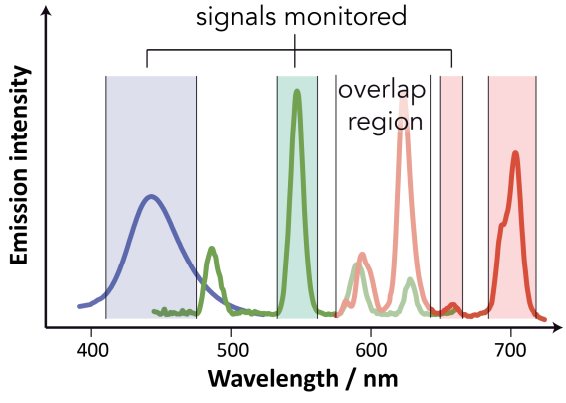

Figure 25. Illustration of coumarin (blue), Tb (green) and Eu (red) emissions monitored in the three color detection experiments.

Protein tyrosine phosphatase 1B (PTP1B) can be regulated by RONS such as H_2O_2.[9,88] The enzyme contains a catalytically active cysteine, which is oxidizable, leading to deactivation of the enzyme.[89] In contrast, β-galactosidase contains an active site glutamate residue which is not oxidizable by H_2O_2. When we performed the same experiment as described above but with β-galactosidase and the interacting analytes PTP1B and H_2O_2, **Tb38Phos** was processed by PTP1B in the absence of H_2O_2 but not in its presence (Figure 26b). This is consistent with the inactivation of PTP1B by H_2O_2. PTP1B turned out to be a generally sensitive enzyme and quite a large **Tb38Phos** concentration (50 μM) was necessary in order to get a robust signal. The reduced Tb emission observed for the β-galactosidase/PTP1B combination compared to only PTP1B added (65% lower) (Figure 26b, column 7 vs. 3), could be due to an inner filter effect[90] from the produced **Eu43**. The small

increase in coumarin emission seen for this galactosidase/PTP1B combination (~2 fold) is presumably a result of residual coumarin emission from **Eu43** and **Tb43**.

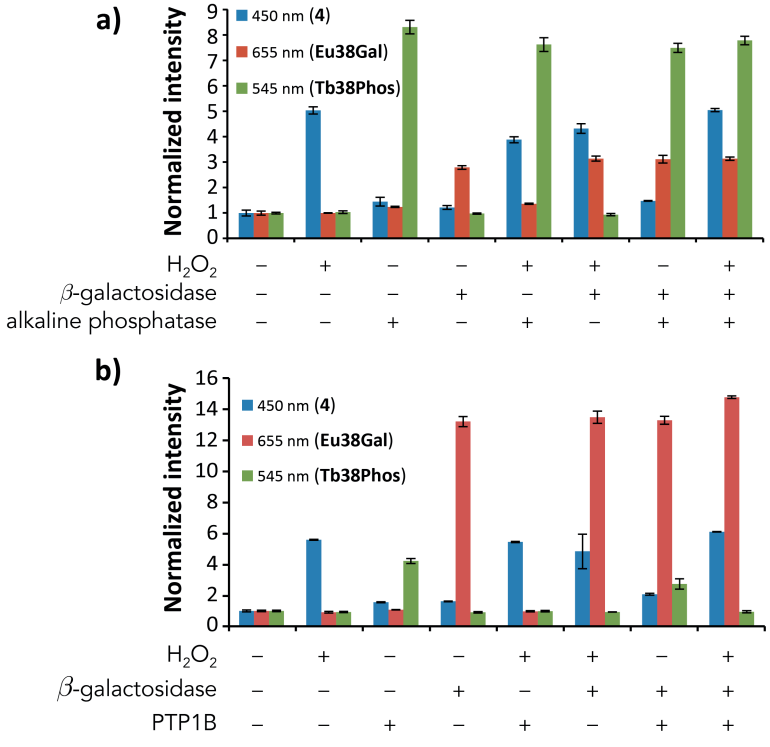

Figure 26. Simultaneous detection of β-galactosidase, H_2O_2 and a) alkaline phosphatase or b) PTP1B. a) ***4*** *(1 μM),* ***Eu38Gal*** *(6.25 μM) and* ***Tb38Phos*** *(12.5 μM), β-galactosidase (0 or 1 U), alkaline phosphatase (0 or 0.2 U), H_2O_2 (0 or 100 μM) 1 h, 37 °C (HEPES 100 mM, NaCl 1 M, $MgCl_2$ 5 mM and $ZnCl_2$ 0.2 mM, pH 8.0). b)* ***4*** *(2 μM), was incubated with β-galactosidase (0 or 0.25 U), PTP1B (0 or ~0.4 mU) and H_2O_2 (0 or 100 μM) for 30 min at 37 °C (HEPES 100 mM, pH 7.0).* ***Eu38Gal*** *(12.5 μM) and* ***Tb38Phos*** *(50 μM) were then added, and incubated at rt for 30 min. Steady state scan: λ_{ex} = 410 nm, λ_{em} = 450 nm, time resolved scan: λ_{ex} = 356 nm, λ_{em} = 545 & 655 nm, 250 μs delay, 1050 μs sample window. Error bars show standard error based on three independent experiments. Intensities are normalized to that of the blank for each probe.*

4.3 Conclusion

A range of Eu- and Tb-based responsive probes have been prepared. The probes gave robust turn-on responses when treated with their analytes. The Ln-based probes could readily be applied to the detection of multiple enzyme activities. Combined with an organic fluorophore detection of two enzymes and a small molecule regulator could be achieved with minimal

spectral cross-talk. The current work represents the first use of Ln-based responsive probes for multicolor detection. It is worth noting that all of the experiments could be performed on a luminescence plate reader, significantly simplifying the experimental setup, and bringing the technique closer to potential end-users. This work represents a significant step forward in multiplex detection, with possible applications in the detection of multiple analytes in a biological setting.

5. Functionalization of lanthanide complexes *via* Cu^{I}-catalyzed azide-alkyne cycloaddition (papers III & IV)

Since its independent discovery by Meldal[79b] and Sharpless[79a] the copper-catalyzed azide-alkyne cycloaddition (CuAAC) has found widespread use as a robust and high yielding ligation reaction. While often viewed as the archetypical click reaction,[91] for some substrates the CuAAC can require considerable optimization in order to proceed at an acceptable rate.[92]

Our own difficulties with this reaction together with literature reports describing its sluggishness for coupling of Ln-partners[93] inspired us to find conditions which would provide a high yielding and operationally simple method to access triazole-linked Ln-antenna compounds. In addition to providing efficient access to different Ln-antenna combinations, this approach can be envisioned for constructing heterobimetallic Ln compounds which can otherwise be challenging because of the very similar chemical properties of the Ln^{III} ions.[35-36] Heterobimetallic Ln complexes are attractive targets as they could potentially be used as multimodal imaging agents (e.g. by combining Gd with any of the luminescent Lns for dual MRI and luminescence imaging).

5.1 Results and discussion

We first prepared the five different Ln complexes **Ln44-48**, and the six coupling partners **A-F** (Scheme 22). The Ln complexes were chosen for one of the following reasons: previous (successful or unsuccessful) employment in this reaction (**Ln44-46**),[55a,93a,b,94] our own use of the complex (**Ln47**) or its usefulness for constructing heterotrimetallic complexes (**La48**).

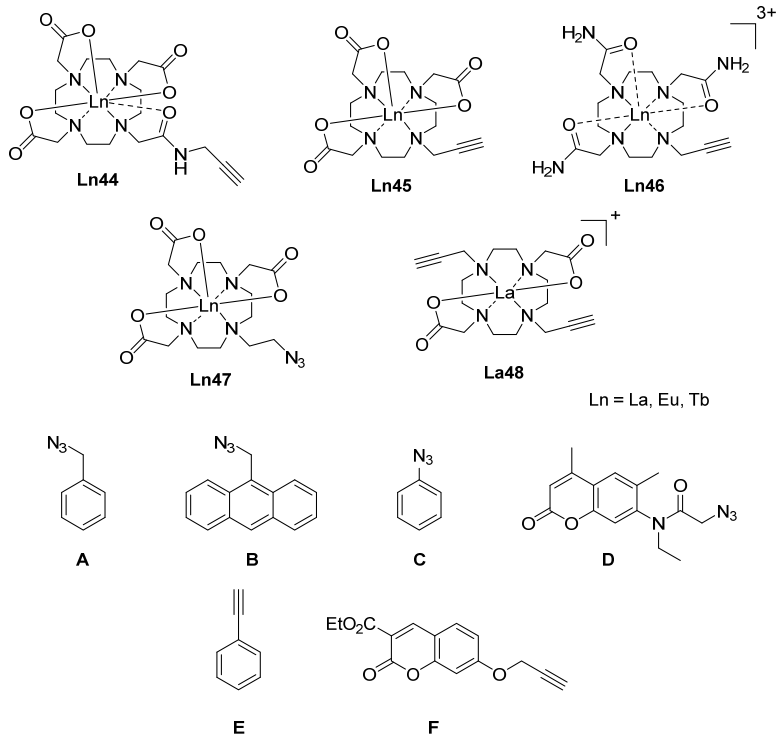

Scheme 22. Ln complexes and coupling partners used in this study.

The Ln complexes **Ln44-48** were synthesized in a fashion similar to that of **Ln47** (Scheme 23a). Monoalkylation of cyclen with **49** followed by trialkylation with *t*-butyl bromoacetate gave the protected DO3A derivative **51** in 58% yield over these two steps. Deprotection in TFA/CH_2Cl_2 and Ln complexation gave the Ln complexes **Ln47**. The dipropargyl complex **La48** was synthesized in three steps from diester **53** (Scheme 23b).[95] Dialkylation of **53** with propargyl bromide followed by *t*-butyl ester deprotection and La complexation gave **La48** in 85% yield over these three steps.

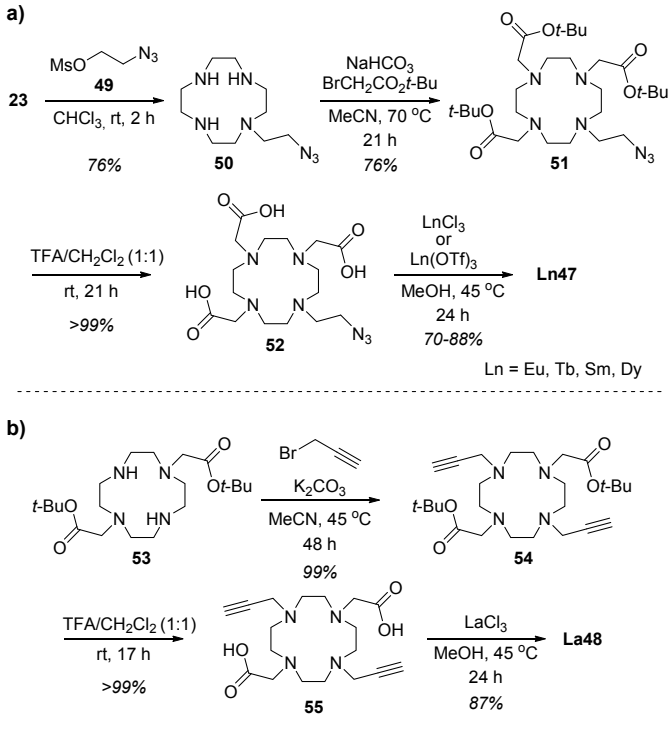

*Scheme 23. Synthesis of **Ln47** and **La48**.*

With these compounds at hand we began the search for efficient coupling conditions. We submitted a mixture of **La45** and **A** or **B** to a number of different combinations of Cu-sources ($CuSO_4$, $Cu(acac)_2$, $Cu(OAc)_2$, $CuBr_2$, CuCl, CuI, Cu_2O), solvents (DMSO, DMF, MeCN, H_2O/*t*-BuOH-mixtures), additives (NaAsc, benzoic acid[96]), ligands (TBTA,[97] TMEDA,[98] DIEA[99]) and temperatures (rt to 120 °C, oil bath or MW heating). We found that CuI (5 mol%) in a MeCN/piperidine or MeCN/*i*-Pr_2NH solvent mixture resulted in full conversion to the product (determined by ^{1}H-NMR, TLC and ESI-MS) after 5 min when heated at 100 °C in a microwave reactor. These conditions are similar to those reported by the Imperiali group for the synthesis of hydroxyquinoline-based kinase sensors.[100] Under the same conditions but with oil bath heating the reaction did not reach full conversion even after 22 h. We next investigated the scope of this reaction.

The reaction was not sensitive to the polarity of the coupling partners. Both the azide- and alkyne-containing Ln complexes reacted in moderate to good yields (Table 5). We were especially pleased to see that even the triamide **Ln46** reacted under these conditions. **Ln46** has been reported to be a difficult substrate for the CuAAC reaction.[93b]

Table 5. Overview of the coupling reactions performed.[a]

Entry	Ln complex	Coupling partner	Time (min)	Yield [precipitation/chromatography (%)]
1	**La44**	**A**	15	85/57
2	**Eu44**	**A**	15	88
3	**La45**	**A**	15	58/66
4	**Eu45**	**A**	15	60/55
5	**Tb45**	**A**	15	56/45
6	**La45**	**C**	30	44
7	**Eu45**	**C**	30	42
8	**Eu45**	**D**	60	95
9	**Tb45**	**D**	60	79
10	**La46**	**A**	15	86
11	**Eu46**	**A**	15	90
12	**La47**	**E**	30	96/16
13	**Eu47**	**E**	30	82/34
14	**Tb47**	**E**	30	79/36
15	**La47**	**F**	30	91/29
16	**Eu47**	**F**	30	98
17	**Tb47**	**F**	30	37/33
18	**La48**	**A**	30	47/44

[a]Reaction conditions: Ln complex (1 equiv.), coupling partner (1.1 equiv.) CuI (5%), *i*-Pr_2NH/MeCN (1:4), 0.2 M, 100 °C, microwave heating.

Since all of the starting Ln complex (which has solubility similar to that of the product) was consumed in the reaction, it was possible to isolate the coupling product by precipitation from the reaction mixture with Et_2O. Pure products (as determined by HPLC) could be obtained in most cases by repeated precipitation from MeOH/Et_2O. Alternatively, the product could be purified by column chromatography by eluting with MeCN/H_2O. When *i*-Pr_2NH was used as a base and the cycloaddition product had good solubility in MeCN/H_2O the two methods gave similar yields. However, when product solubility was low in MeCN/H_2O, precipitation gave superior yields (Table 5, entries 12−15).

We were also interested to see whether these conditions could be used for the rational preparation of heterobimetallic Ln complexes. **Ln60** was prepared in four steps from **53** (Scheme 24). Alkylation of **53** with coumarin **56** and propargyl bromide gave compound **58**. Cleavage of the *t*-butyl esters, followed by Ln complexation gave **Ln60** in a total yield of 49% over all four steps.

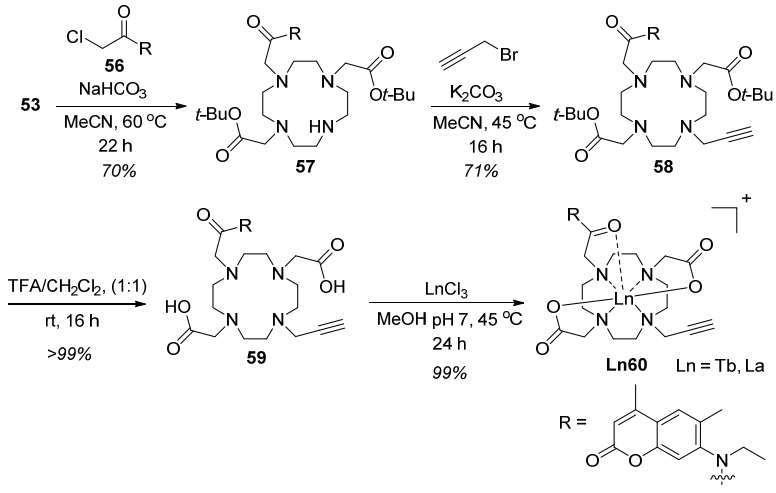

*Scheme 24. Synthesis of **Ln60**.*

The reaction of **Ln60** with **Eu47** gave the expected heterobimetallic complexes **TbEu61** and **LaEu61** in 60% and 33% isolated yield after column chromatography (Scheme 25). In addition, we could prepare the trimetallic compound **LaEu$_2$62** in 34% isolated yield by double ligation of **La48** with **Eu47** (Scheme 25). ESI-MS analysis showed the presence of only the molecule ion peak with the expected isotope distribution pattern.

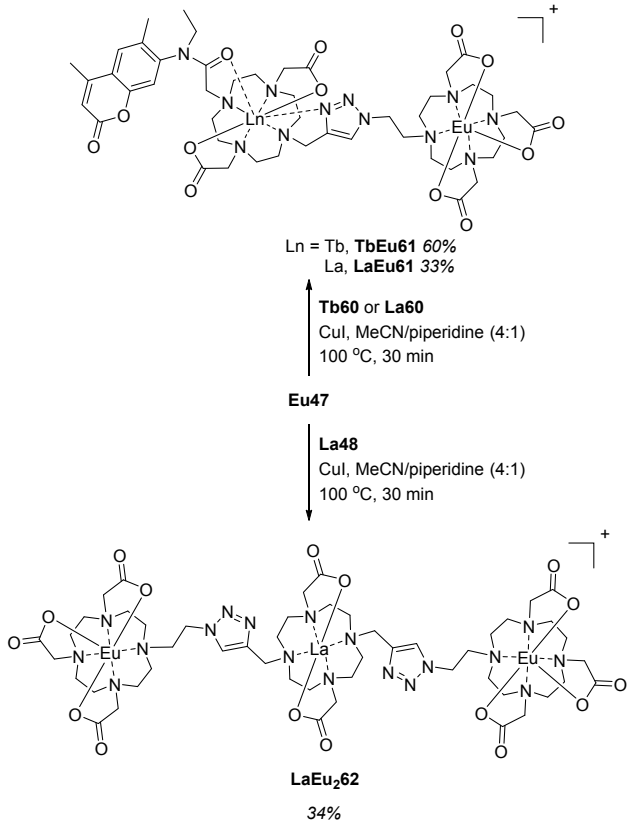

Scheme 25. Synthesis of heterometallic Ln complexes.

5.1.1 Expanding the scope to sensitive substrates

While these conditions work well for robust compounds, they are quite harsh, and not generally suited for more labile substrates. For instance, these conditions do not work well for the caged coumarin precursors **21**, described in Chapters 3 and 4. However, there was clearly a need to improve the performance of this reaction for these types of substrates, as the initial conditions we used were prohibitively slow (see Chapter 3). As such, we set out to find efficient and mild conditions for this reaction. For the following screening **Tb47** and **21Bn** were used as coupling partners and the reactions were performed at room temperature.

A number of different solvent were screened (H_2O, MeOH, MeCN, H_2O/MeOH, H_2O/MeCN, piperidine/MeCN and DMSO). We were initially reluctant to use DMSO as solvent due to the difficulty of removing it. Nevertheless, it turned out to work best, presumably due to its superior ability to effectively solubilize all reaction partners.

Key to the efficient performance of the reaction was the realization that a large excess of NaAsc was necessary. Catalytically active Cu^{I} is colorless while Cu^{II} is blue. The reaction mixture was blue or greenish-blue until at least 6 equiv. of NaAsc was added, at which point it turned yellow indicating the absence of Cu^{II}.

Cu-coordinating ligands can increase the rate of the CuAAC reaction by several orders of magnitude.[97,101] The role of the ligand can be multifold: to protect the catalytically active Cu^{I} species towards oxidation, to alter the equilibrium concentrations of various Cu-clusters present in the reaction mixture as well as direct involvement in the catalytic cycle.[92] To test the effect of ligands in this coupling we prepared TBTA,[97] THPTA[102] and $BimPy_2$[101b] shown in Scheme 26.

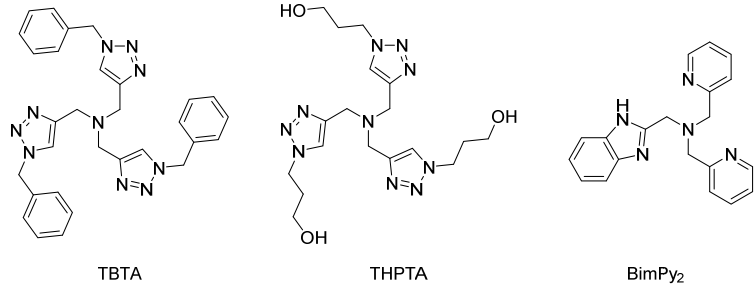

Scheme 26. The different ligands used in the optimization.

A screen of ligands using these conditions is shown in Table 6. $BimPy_2$ proved to be most efficient, yielding **Tb38Bn** in 84% yield after 20 h. After the reaction the DMSO could be removed by repeated precipitation of the product from MeOH/Et_2O. **Tb38Bn** could then be further purified by silica column chromatography using MeCN/H_2O as eluent.

Table 6. A selection of the conditions tried in the CuAAC screening.

Entry	NaAsc	Ligand	Yield (%)
1	−	−	2
2	+	−	16
3	+	TBTA	31
4	+	THPTA	60
5	+	$BimPy_2$	84

All reactions were performed on a 0.02 mmol scale, **Tb47** (1.1 equiv.) **21Bn** (1 equiv.), CuOAc (0.1 equiv) and NaAsc (6.5 equiv.), ligand [0.2 equiv. (TBTA, THPTA) or 0.1 equiv. ($BimPy_2$)], DMSO, rt, 20 h. Yields were determined by HPLC.

5.2 Photophysical characterization

All complexes gave Ln-centered emission when excited through their aromatic moieties. The heterobimetallic **TbEu61** showed dual Eu and Tb emission (Figure 27). The luminescent lifetimes (τ) of all the complexes were determined in H_2O and D_2O and are summarized in Table 7 along with the hydration states (q).

Table 7. Luminescent lifetimes and hydration states of selected products

Complex (nm, $\lambda_{ex}/\lambda_{em}$)	τ_{H_2O} (ms)	τ_{D_2O} (ms)	q
Eu45C (280/590)	1.17	2.83	0.3
Eu45D (280/590)	1.13	2.46	0.3
Tb45D (280/543)	3.54	2.70	0.1
Eu46A (266/614)	1.10	1.64	−0.3
Eu47 (397/590)	0.61	4.28	1.4
Tb47 (366/488)	0.87	1.66	2.4
Eu47E (278/615)	1.26	2.22	0.1
Tb47E (278/546)	2.12	3.13	0.5
Eu47F (356/614)	0.93	2.75	0.4
Tb47F (356/543)	0.41	2.15	9.7
Tb60 (320/544)	0.58	0.72	1.4
TbEu61			
(328/699)	1.03	2.67	0.4
(328/545)	0.68	0.74	0.3
LaEu61 (328/699)	1.18	2.62	0.3
$LaEu_2$62 (396/699)	0.52	1.49	1.2

Previous reports have established that triazole formation leads to the displacement of one coordinating water molecule in **Ln45** type complexes.[93a,b,103] Our results agree with this, as the **Ln45**-derivatives have q = 0.1−0.3. The q values of the **Ln47** series indicated a similar change in coordination environment, with q = 1.4−2.4 (**Ln47**) before and q = 0.1−0.5 (**Ln47E** and **Eu47F**) after triazole formation. The q = 9.7 for **Tb47F** may indicate energy back transfer from Tb to the coumarin antenna.

A further indication of a change in coordination environment upon triazole formation was gained from inspecting the shape of the Eu emission spectrum. The hypersensitive Eu $^5D_0 \rightarrow {}^7F_2$ (614 nm) transition is very sensitive to changes in coordination environment.[104] By comparing this transition to the $^5D_0 \rightarrow {}^7F_1$ (590 nm) transition, which is essentially unaffected by the Eu environment, information on the coordination environment can be gained.[104] The ratio of these transitions (I^{614}/I^{590}) increased from 1.10 in **Eu47** to 1.47 for **Eu47E** and 3.13 for **Eu47F**.

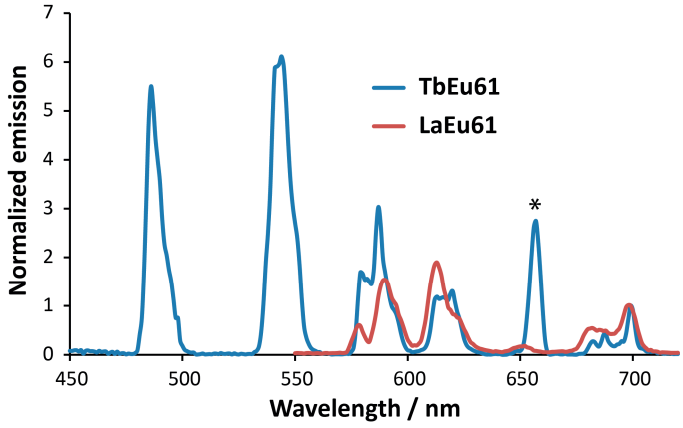

*Figure 27. Normalized emission spectra of **TbEu61** (blue) and **LaEu61** (red) upon antenna-centered excitation (λ_{ex} = 328 nm, steady state). The peak marked with an asterisk is due to scattered light. The spectrum of **TbEu61** has been subjected to a baseline correction function to remove residual coumarin emission.*

5.3 Conclusion

Two different sets of conditions for the preparation of triazole-linked Ln-antenna complexes have been developed. For robust substrates microwave heating significantly increased the rate of the reaction. The utility of these conditions for Ln complex synthesis was demonstrated by preparing hetero bi- and trimetallic Ln complexes. Such complexes could potentially be used as multimodal imaging agents. Furthermore, conditions for the coupling of more sensitive substrates with Ln-partners were found.

Concluding remarks

The study of interconnected biological processes in real time remains a major challenge. The work presented in this thesis demonstrates that Ln-based luminescent probes can provide a valuable addition to the biochemist's toolbox. While we have not yet investigated the possibility of multicolor detection *in vivo* with our probes, future work will focus on realizing this goal.

The different probes presented in this thesis have their various strengths. The 1st generation probes provide the highest brightness and the capability for ratiometric detection. However, the pH dependence of their emission, while attractive in certain situations, is not always desirable. By altering the design, we were able to remove the pH dependence of emission and increase the dynamic range of the probes significantly (from ~6-fold to 50-fold). In addition, the new design enabled sensitization of both Tb and Eu.

This thesis presents the first examples of the use of responsive Ln-based probes in multicolor imaging. The work represents a significant step forward in multiplex detection, with possible applications in the detection of multiple analytes in a biological setting. Future work in this area will focus on expanding the probe palette by developing antennae capable of sensitizing additional Lns.

Svensk sammanfattning

Vi lever i en värld där mycket av det som sker är dolt för oss. Dolt på grund av våra sinnens begränsningar, vilket gör oss oförmögna att se mycket små så väl som mycket stora fenomen. Människans nyfikenhet har drivit på utvecklingen av verktyg som låter oss gå bortom denna begränsning. Dessa inkluderar instrument för att observera hela spektrat från stjärnor och galaxer (teleskop) till naturens minsta byggstenar (partikelacceleratorer). Mellan dessa extremer finns atomer och molekyler, vars interaktioner styr cellers funktion och uppbyggnad. Celler räknas ofta som de minsta *levande* byggstenarna men är trots detta enormt komplexa, med en förmåga att styra och samverka miljontals reaktioner varje sekund. Med denna komplexitet i åtanke är det lätt att förstå svårigheten att följa enskilda processer på cellnivå.

En av de främsta metoder som har vuxit fram för att göra just det kallas ”luminescence imaging” (LI). LI ger möjlighet att visualisera cellulära händelser med stor precision. För att upptäcka en specifik molekyl (som ofta benämns analyt) eller process med hjälp av LI så används en spektrofotometer tillsammans med en speciellt framtagen luminescerande molekyl (en molekyl som absorberar och emitterar ljus), ofta kallad luminescerande prob. Luminescerande prober är molekyler som i kontakt med sitt analyt får förändrade fotofysiska egenskaper, vilket kan detekteras med hjälp av en spektrofotometer.

Den här avhandlingen beskriver utvecklandet av luminiscerande prober som kan användas för att detektera förskomsten av små (bio)molekyler och enzym. Gemensamt för de prober som presenteras här är att de i sin struktur inkluderar en lantanoid. Lantanoiderna är grundämnen i periodiska systemets f-block. Dessa har en rad fotofysiska egenskaper som gör dem attraktiva att använda i luminescerande prober, såsom smala, väldefinierade emissionsband, och långa livstider i sitt exciterade tillstånd. Lantanoider är dock mycket dåliga på att absorbera ljus. För att komma runt detta problem kan en organisk kromofor (en molekyl som effektivt absorberar ljus) kopplas samman med lantanoiden. Då kan istället kromoforen exciteras, varpå den kan överföra exciteringsenergin till lantanoiden, som i sin tur emitterar.

De prober vi har utvecklat består av en kumarin (kromoforen) som är kopplad till ett lantanoidkomplex, där Eu eller Tb är de lantanoider som vi framgångsrikt kunnat använda. Kumarinen är i sin tur kopplad till en skyddsgrupp som kan klyvas av ett specifikt analyt. Resultatet av denna ana-

lyttriggade klyvning av skyddsgruppen är att kumarinens, och i förlängningen, lantanoidens fotofysiska egenskaper förändras. Detta i sin tur leder till en förändring i emittans när processen studeras med hjälp av en spektrofotometer. Genom att välja skyddsgrupper som kemoselektivt klyvs av en specifik analyt så kan denna metod användas för att studera denna analyt i närvaro av andra molekyler.

I kapitel 3 och 4 i avhandlingen beskrivs en variant av ovanstående metod, där vi istället för att koppla skyddsgruppen direkt till en kumarin har kopplat den till en *kumarinprekursor*. Analyttriggad klyvning av skyddsgruppen leder i det här fallet till *bildandet* av en kumarin (Figur 1). Detta leder i sin tur till en påslagning av emittansen när processen följs med en spektrofotometer.

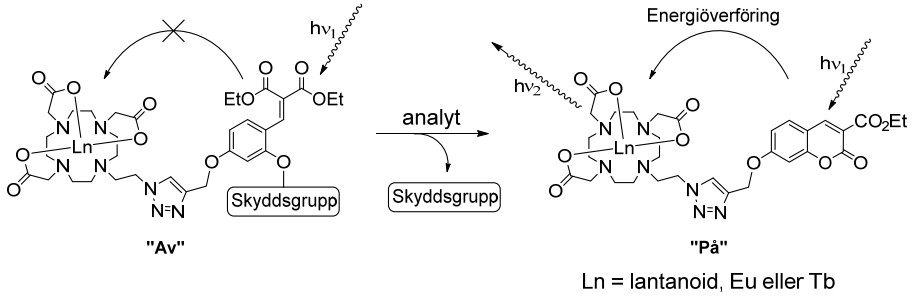

Figur 1. Principen bakom några av de prober som beskrivs i avhandlingen.

Vi har använt den här strategin för att konstruera prober som kan detektera en rad olika analyt: fluoridjoner, palladium, väteperoxid samt en mängd enzym (β-galaktosidas, β-glukosidas, α-mannosidas och fosfatas). Avhandlingen beskriver dock inte bara syntesen av dessa prober. Vi har också använt dem, bland annat för att studera enzym (β-galaktosidas) i levande bakterier, men också för att detektera flera analyter samtidigt. Genom att använda både en Eu- och en Tb-baserad prob har vi lyckats detektera två olika analyt samtidigt, något som aldrig förut gjorts med lantanoidbaserade prober. Vi kunde dessutom utöka detta till att detektera tre analyt samtidigt, genom att, utöver dessa prober också använda en kumarinbaserad prob.

Avhandlingen representerar ett signifikant bidrag mot målet att precist kunna studera sammankopplade processer i celler. Något som är av stor vikt för en ökad förståelse kring mekanismer bakom sjukdomstillstånd, vilket i förlängningen kan leda till nya läkemedel.

Appendix

Reprints were made with permission from the respective publishers.

I Szíjjártó, C., Pershagen, E., Ilchenko, N. O., Borbas, K. E. *Chem. – Eur. J.* **2013**, *19*, 3099–3109.

II Pershagen, E., Nordholm, J., Borbas, K. E. *J. Am. Chem. Soc.* **2012**, *134*, 9832–9834.

III Pershagen, E., Borbas, K. E. *Angew. Chem. Int. Ed.* DOI: 10.1002/anie.201408560R1

IV Szíjjártó, C., Pershagen, E., Borbas, K. E. *Dalton Trans.* **2012**, *41*, 7660–7669.

Acknowledgements

This thesis would not have been possible without the help and support from a number of people.

My supervisor *Eszter Borbas* for accepting me as a PhD student. I am very grateful for all your help and support. I am very pleased to have spent my PhD working with this exciting chemistry. You are a great supervisor!

My collaborator and coworker *Csongor Szíjjártó* for all the help with the projects and for being a great guy in and outside of the lab.

My collaborators *Johan Nordholm* and *Robert Daniels*, thank you for teaching me some of the tips and tricks of biochemistry.

Julien Andres for invaluable help with photophysical measurements.

The proofreaders of this thesis – *Eszter Borbas*, *Ylva Wikmark*, *Julien Andres*, *Sashiprabha Vithanarachchi*, *Lukasz Pilarski*, *Joel Malmgren* and *Susanne Pershagen.*

The Borbas group – *Ruisheng Xiong, Julien Andres, Sashiprabha Vithanarachchi* and *Anna Arkhypchuk*.

Helena Grennberg for taking the time to read my thesis.

Past members of the Borbas group, especially *Johanna Laakso*, *Carina Sollert*, *Cornelia Ahlström*, *Aron Luthman* and *Nadiya Ilchenko* and *Derar Issa Al-Smadi,* for creating a nice working atmosphere.

Joel Malmgren for super fun times.

Richard Lihammar – thank you for driving me through California!

Elina Buitrago, Nazli Jalalian, Fredrik Tinnis, Ylva Wikmark, Richard Lihammar, Anuja Nagendiran, Joel Malmgren, Helena Lundberg and *Alexey Volkov* for awesome conference trips.

Marcin Kalek for valuable discussions on kinetics measurements.

The TA staff, especially *Karin Larsson* for all your help with troubleshooting the HPLC.

Mikael Olivenberg for giving me access to your stopped flow instrument and *Lisa Lang* for instructing me on its use.

Gunnar von Heijne for access to a plate reader.

All the people lending me chemicals over the years.

All the people at the Stockholm University organic chemistry department.

Knut och Alice Wallenbergs stiftelse, *Ångpanneföreningen*, *Kungliga Skogs och Lantbruksakademien*, *Lennanders Stiftelse, Gålöstiftelsen* and *Helge Axon Johnsons Stiftelse* for financial support.

Min familj, för att ni alltid finns där.

Gustav för din villkorslösa vänskap.

Länsögänget – you know who you are!

Min hustru *Ylva.* Jag älskar dig.

References

[1] J. S. Dodd, Editor, *The ACS Style Guide: A Manual for Authors and Editors, Second Edition*, ACS, **1997**.

[2] A. J. Bruce Alberts, Julian Lewis, Martin Raff, Keith Roberts, Peter Walter, *Molecular Biology of the Cell, 4th Edition*, 4 ed., Garland Science, New York, N. Y., **2002**.

[3] B. Valeur, *Molecular Fluorescence - An Introduction: Principles and Applications, 1st Edition*, Wiley-VCH, **2000**.

[4] IUPAC Gold Book: http://goldbook.iupac.org/L03649.html accessed 221114

[5] a) J. Chan, S. C. Dodani, C. J. Chang, *Nature Chem.* **2012**, *4*, 973-984; b) L. D. Lavis, R. T. Raines, *ACS Chem. Biol.* **2008**, *3*, 142-155.

[6] N. A. C. Jane B. Reece, Lisa A. Urry, Michael L. Cain, Steven A. Wasserman, Peter V. Minorsky, Robert B. Jackson, *Campbell Biology, 9th Edition*, 9 ed., Benjamin Cummings, **2012**.

[7] M. M. C. David L. Nelson, *Lehninger Principles of Biochemistry, 4th Edition*, 4 ed., W. H. Freeman, **2004**.

[8] a) J. Stebbing, L. C. Lit, H. Zhang, R. S. Darrington, O. Melaiu, B. Rudraraju, G. Giamas, *Oncogene* **2014**, *33*, 939-953; b) N. K. Tonks, B. G. Neel, *Cell* **1996**, *87*, 365-368.

[9] A. Östman, J. Frijhoff, Å. Sandin, F.-D. Böhmer, *J. Biochem.* **2011**, *150*, 345-356.

[10] a) C. C. Winterbourn, *Nat. Chem. Biol.* **2008**, *4*, 278-286; b) B. C. Dickinson, C. J. Chang, *Nat. Chem. Biol.* **2011**, *7*, 504-511.

[11] K. Ohtsubo, J. D. Marth, *Cell* **2006**, *126*, 855-867.

[12] P. Atkins, J. de Paula, *Atkins' Physical Chemistry, 8th Edition*, Oxford University Press, **2006**.

[13] A. Jablonski, *Nature* **1933**, *131*, 839-840.

[14] E. V. Anslyn, D. A. Dougherty, *Modern Physical Organic Chemistry, 1st Edition*, 1 ed., University Science, **2006**.

[15] a) J. Franck, E. G. Dymond, *T. Faraday. Soc.* **1926**, *21*, 536-542; b) E. Condon, *Phys. Rev.* **1926**, *28*, 1182-1201.

[16] This includes vibrational sublevels of the triplet state.

[17] P. Atkins, J. de Paula, *Elements of Physical Chemistry, 4th Edition*, **2005**.

[18] J. R. Lakowicz, *Principles of Fluorescence Spectroscopy*, Plenum Press, **2006**.

[19] E. Brooks Shera, N. K. Seitzinger, L. M. Davis, R. A. Keller, S. A. Soper, *Chem. Phys. Lett.* **1990**, *174*, 553-557.
[20] a) E. Betzig, G. H. Patterson, R. Sougrat, O. W. Lindwasser, S. Olenych, J. S. Bonifacino, M. W. Davidson, J. Lippincott-Schwartz, H. F. Hess, *Science* **2006**, *313*, 1642-1645; b) T. A. Klar, S. Jakobs, M. Dyba, A. Egner, S. W. Hell, *Proc. Natl. Acad. Sci. U. S. A.* **2000**, *97*, 8206-8210.
[21] IUPAC defines the Stokes shift as the difference between the band maxima of absorption and luminescence arising from the same electronic transition.
[22] G. G. Stokes, *Philos. Trans. R. Soc. London, Ser. A* **1852**, *142*, 463-562.
[23] J. V. Frangioni, *Curr. Opin. Chem. Biol.* **2003**, *7*, 626-634.
[24] A. M. Smith, M. C. Mancini, S. Nie, *Nat. Nanotechnol.* **2009**, *4*, 710-711.
[25] A turn-on response is desirable since it offers greater selectivity. The greater selectivity stems from the fact that any process which destroys the probe will lead to a decrease in emission intensity.
[26] Y. Yang, Q. Zhao, W. Feng, F. Li, *Chem. Rev.* **2012**, *113*, 192-270.
[27] M. E. Jun, B. Roy, K. H. Ahn, *Chem. Commun.* **2011**, *47*, 7583-7601.
[28] A. Minta, J. P. Y. Kao, R. Y. Tsien, *J. Biol. Chem.* **1989**, *264*, 8171-8178.
[29] K. R. Gee, Z. L. Zhou, D. Ton-That, S. L. Sensi, J. H. Weiss, *Cell Calcium* **2002**, *31*, 245-251.
[30] a) Y. Gabe, Y. Urano, K. Kikuchi, H. Kojima, T. Nagano, *J. Am. Chem. Soc.* **2004**, *126*, 3357-3367; b) H. Peng, Y. Cheng, C. Dai, A. L. King, B. L. Predmore, D. J. Lefer, B. Wang, *Angew. Chem. Int. Ed.* **2011**, *50*, 9672-9675; c) G. Chen, D. J. Yee, N. G. Gubernator, D. Sames, *J. Am. Chem. Soc.* **2005**, *127*, 4544-4545; d) K. R. Gee, W.-C. Sun, M. K. Bhalgat, R. H. Upson, D. H. Klaubert, K. A. Latham, R. P. Haugland, *Anal. Biochem.* **1999**, *273*, 41-48.
[31] D. W. Domaille, E. L. Que, C. J. Chang, *Nat. Chem. Biol.* **2008**, *4*, 168-175.
[32] H. Kobayashi, M. Ogawa, R. Alford, P. L. Choyke, Y. Urano, *Chem. Rev.* **2010**, *110*, 2620-2640.
[33] This refers to the pseudo-Stokes shifts observed in Ln-antenna complexes.
[34] N. N. Greenwood, A. Earnshaw, *Chemistry of the Elements, 2nd Edition*, Butterworth-Heinemann, **1997**.
[35] S. A. Cotton, *Lanthanide and Actinide Chemistry*, 1 ed., John Wiley & Sons Ltd, **2006**.
[36] S. A. Cotton, in *Encyclopedia of Inorganic and Bioinorganic Chemistry*, John Wiley & Sons, Ltd, **2011**.
[37] S. V. Eliseeva, J.-C. G. Bunzli, *Chem. Soc. Rev.* **2010**, *39*, 189-227.

[38] J.-C. G. Bünzli, C. Piguet, *Chem. Soc. Rev.* **2005**, *34*, 1048-1077.
[39] M. C. Heffern, L. M. Matosziuk, T. J. Meade, *Chem. Rev.* **2014**, *114*, 4496-4539.
[40] J.-C. G. Bünzli, *Chem. Rev.* **2010**, *110*, 2729-2755.
[41] a) A. Beeby, I. M. Clarkson, R. S. Dickins, S. Faulkner, D. Parker, L. Royle, A. S. de Sousa, J. A. G. Williams, M. Woods, *J. Chem. Soc. Perk. Trans. 2* **1999**, 493-504; b) W. D. Horrocks, D. R. Sudnick, *J. Am. Chem. Soc.* **1979**, *101*, 334-340.
[42] J.-C. G. Bünzli, *Chem. Rev.* **2010**, *110*, 2729-2755.
[43] a) S. I. Weissman, *J. Chem. Phys.* **1942**, *10*, 214-217; b) P. Yuster, S. I. Weissman, *J. Chem. Phys.* **1949**, *17*, 1182-1188.
[44] A. Bodi, K. E. Borbas, J. I. Bruce, *Dalton Trans.* **2007**, 4352-4358.
[45] a) T. Terai, Y. Urano, S. Izumi, H. Kojima, T. Nagano, *Chem. Commun.* **2012**, *48*, 2840-2842; b) M. H. V. Werts, J. W. Hofstraat, F. A. J. Geurts, J. W. Verhoeven, *Chem. Phys. Lett.* **1997**, *276*, 196-201; c) M. H. V. Werts, J. W. Verhoeven, J. W. Hofstraat, *J. Chem. Soc. Perk. Trans. 2* **2000**, 433-439; d) W. Huang, D. Wu, D. Guo, X. Zhu, C. He, Q. Meng, C. Duan, *Dalton Trans.* **2009**, 2081-2084; e) M. H. V. Werts, R. H. Woudenberg, P. G. Emmerink, R. van Gassel, J. W. Hofstraat, J. W. Verhoeven, *Angew. Chem.* **2000**, *112*, 4716-4718; f) S. I. Klink, P. O. Alink, L. Grave, F. G. A. Peters, J. W. Hofstraat, F. Geurts, F. C. J. M. van Veggel, *J. Chem. Soc. Perk. Trans. 2* **2001**, 363-372.
[46] a) D. Parker, J. Yu, *Chem. Commun.* **2005**, 3141-3143; b) P. Atkinson, K. S. Findlay, F. Kielar, R. Pal, D. Parker, R. A. Poole, H. Puschmann, S. L. Richardson, P. A. Stenson, A. L. Thompson, J. Yu, *Org. Biomol. Chem.* **2006**, *4*, 1707-1722.
[47] a) B. Song, G. Wang, M. Tan, J. Yuan, *J. Am. Chem. Soc.* **2006**, *128*, 13442-13450; b) B. Song, G. Wang, J. Yuan, *Chem. Commun.* **2005**, 3553-3555.
[48] a) M. S. Tremblay, M. Halim, D. Sames, *J. Am. Chem. Soc.* **2007**, *129*, 7570-7577; b) T. Terai, K. Kikuchi, Y. Urano, H. Kojima, T. Nagano, *Chem. Commun.* **2012**, *48*, 2234-2236.
[49] a) G. F. de Sa, O. L. Malta, D. C. de Mello, A. M. Simas, R. L. Longo, P. A. Santa-Cruz, E. F. da Silva, Jr., *Coord. Chem. Rev.* **2000**, *196*, 165-195; b) P. Haenninen, H. Haermae, Editors, *Lanthanide Luminescence: Photophysical, Analytical and Biological Aspects. [In: Springer Ser. Fluoresc., 2011; 7]*, Springer GmbH, **2011**; c) M. Kleinerman, *J. Chem. Phys.* **1969**, *51*, 2370-2381.
[50] Even if singlet sensitization operates the triplet state needs to be sufficiently well separated from the Ln emissive state to prevent energy back transfer and non-radiative quenching of the excited state.
[51] Strictly speaking this is not a Stokes shift, as defined by IUPAC, since the luminescence arises from a different electronic transition

than the absorption. The wavelength difference between sensitizer absorption and lanthanide emission is therefore sometimes referred to as a "pseudo-Stokes shift".

[52] a) B. Song, C. D. B. Vandevyver, A.-S. Chauvin, J.-C. G. Bünzli, *Org. Biomol. Chem.* **2008**, *6*, 4125-4133; b) K. A. White, D. A. Chengelis, K. A. Gogick, J. Stehman, N. L. Rosi, S. Petoud, *J. Am. Chem. Soc.* **2009**, *131*, 18069-18071.

[53] E. Pershagen, K. E. Borbas, *Coord. Chem. Rev.* **2014**, *273-274*, 30-46.

[54] a) Y. Bretonniere, M. J. Cann, D. Parker, R. Slater, *Org. Biomol. Chem.* **2004**, *2*, 1624-1632; b) R. Pal, D. Parker, L. C. Costello, *Org. Biomol. Chem.* **2009**, *7*, 1525-1528; c) D. Parker, R. S. Dickins, H. Puschmann, C. Crossland, J. A. K. Howard, *Chem. Rev.* **2002**, *102*, 1977-2010.

[55] a) R. F. H. Viguier, A. N. Hulme, *J. Am. Chem. Soc.* **2006**, *128*, 11370-11371; b) K. Lee, V. Dzubeck, L. Latshaw, J. P. Schneider, *J. Am. Chem. Soc.* **2004**, *126*, 13616-13617.

[56] a) A. P. de Silva, H. Q. N. Gunaratne, T. E. Rice, *Angew. Chem. Int. Ed.* **1996**, *35*, 2116-2118; b) D. Parker, P. K. Senanayake, J. A. G. Williams, *J. Chem. Soc. Perk. Trans. 2* **1998**, 2129-2139; c) T. Gunnlaugsson, D. A. MacDonaill, D. Parker, *J. Am. Chem. Soc.* **2001**, *123*, 12866-12876; d) T. Gunnlaugsson, J. P. Leonard, K. Senechal, A. J. Harte, *J. Am. Chem. Soc.* **2003**, *125*, 12062-12063.

[57] a) A. P. de Silva, H. Q. N. Gunaratne, T. E. Rice, S. Stewart, *Chem. Commun.* **1997**, 1891-1892; b) O. Reany, T. Gunnlaugsson, D. Parker, *Chem. Commun.* **2000**, 473-474; c) K. Hanaoka, K. Kikuchi, H. Kojima, Y. Urano, T. Nagano, *J. Am. Chem. Soc.* **2004**, *126*, 12470-12476; d) A. Thibon, V. C. Pierre, *J. Am. Chem. Soc.* **2009**, *131*, 434-435; e) E. A. Weitz, V. C. Pierre, *Chem. Commun.* **2011**, *47*, 541-543; f) M. Andrews, J. E. Jones, L. P. Harding, S. J. A. Pope, *Chem. Commun.* **2011**, *47*, 206-208; g) S. J. A. Pope, R. H. Laye, *Dalton Trans.* **2006**, 3108-3113.

[58] a) O. S. Wolfbeis, A. Duerkop, M. Wu, Z. Lin, *Angew. Chem. Int. Ed.* **2002**, *41*, 4495-4498; b) B. Song, G. Wang, M. Tan, J. Yuan, *J. Am. Chem. Soc.* **2006**, *128*, 13442-13450; c) D. R. Kauffman, C. M. Shade, H. Uh, S. Petoud, A. Star, *Nature Chem.* **2009**, *1*, 500-506; d) S. E. Page, K. T. Wilke, V. C. Pierre, *Chem. Commun.* **2010**, *46*, 2423-2425; e) C. Song, Z. Ye, G. Wang, J. Yuan, Y. Guan, *Chem. Eur. J.* **2010**, *16*, 6464-6472; f) A. R. Lippert, T. Gschneidtner, C. J. Chang, *Chem. Commun.* **2010**, *46*, 7510-7512; g) Y. Chen, W. Guo, Z. Ye, G. Wang, J. Yuan, *Chem. Commun.* **2011**, *47*, 6266-6268.

[59] a) R. S. Dickins, S. Aime, A. S. Batsanov, A. Beeby, M. Botta, J. I. Bruce, J. A. K. Howard, C. S. Love, D. Parker, R. D. Peacock, H. Puschmann, *J. Am. Chem. Soc.* **2002**, *124*, 12697-12705; b) P. Atkinson, Y. Bretonniere, D. Parker, *Chem. Commun.* **2004**, 438-

439; c) P. Atkinson, B. S. Murray, D. Parker, *Org. Biomol. Chem.* **2006**, *4*, 3166-3171; d) R. A. Poole, F. Kielar, S. L. Richardson, P. A. Stenson, D. Parker, *Chem. Commun.* **2006**, 4084-4086; e) T. Terai, K. Kikuchi, S.-y. Iwasawa, T. Kawabe, Y. Hirata, Y. Urano, T. Nagano, *J. Am. Chem. Soc.* **2006**, *128*, 6938-6946; f) B. K. McMahon, T. Gunnlaugsson, *J. Am. Chem. Soc.* **2012**, *134*, 10725-10728; g) H. Akiba, J. Sumaoka, M. Komiyama, *Chem. Eur. J.* **2010**, *16*, 5018-5025; h) H. Akiba, J. Sumaoka, M. Komiyama, *ChemBioChem* **2009**, *10*, 1773-1776.

[60] M. Halim, M. S. Tremblay, S. Jockusch, N. J. Turro, D. Sames, *J. Am. Chem. Soc.* **2007**, *129*, 7704-7705.

[61] a) K. E. Borbas, J. I. Bruce, *Chem. Commun.* **2006**, 4596-4598; b) M. P. Oude Wolbers, F. C. J. M. van Veggel, F. G. A. Peters, E. S. E. van Beelen, J. W. Hofstraat, F. A. J. Geurts, D. N. Reinhoudt, *Chem. Eur. J.* **1998**, *4*, 772-780.

[62] E. J. New, D. Parker, D. G. Smith, J. W. Walton, *Curr. Opin. Chem. Biol.* **2010**, *14*, 238-246.

[63] a) W. R. Sherman, E. Robins, *Carbohydr. Res.* **1968**, *7*, 184-192; b) M. Lee, N. G. Gubernator, D. Sulzer, D. Sames, *J. Am. Chem. Soc.* **2010**, *132*, 8828-8830; c) S. Mizukami, S. Watanabe, Y. Hori, K. Kikuchi, *J. Am. Chem. Soc.* **2009**, *131*, 5016-5017.

[64] a) A. R. Lippert, G. C. Van de Bittner, C. J. Chang, *Acc. Chem. Res.* **2011**, *44*, 793-804; b) G. C. Van de Bittner, E. A. Dubikovskaya, C. R. Bertozzi, C. J. Chang, *Proc. Natl. Acad. Sci. U. S. A.* **2010**, *107*, 21316-21321; c) A. R. Lippert, T. Gschneidtner, C. J. Chang, *Chem. Commun.* **2010**, *46*, 7510-7512; d) E. W. Miller, A. E. Albers, A. Pralle, E. Y. Isacoff, C. J. Chang, *J. Am. Chem. Soc.* **2005**, *127*, 16652-16659; e) E. W. Miller, O. Tulyanthan, E. Y. Isacoff, C. J. Chang, *Nat. Chem. Biol.* **2007**, *3*, 263-267; f) M. C. Y. Chang, A. Pralle, E. Y. Isacoff, C. J. Chang, *J. Am. Chem. Soc.* **2004**, *126*, 15392-15393; g) A. E. Albers, V. S. Okreglak, C. J. Chang, *J. Am. Chem. Soc.* **2006**, *128*, 9640-9641; h) B. C. Dickinson, C. J. Chang, *J. Am. Chem. Soc.* **2008**, *130*, 9638-9639; i) D. Srikun, E. W. Miller, D. W. Domaille, C. J. Chang, *J. Am. Chem. Soc.* **2008**, *130*, 4596-4597; j) B. C. Dickinson, C. Huynh, C. J. Chang, *J. Am. Chem. Soc.* **2010**, *132*, 5906-5915.

[65] A. Warnecke, in *Drug Delivery in Oncology*, Wiley-VCH Verlag GmbH & Co. KGaA, **2011**, pp. 553-589.

[66] J. L. M. Jourden, K. B. Daniel, S. M. Cohen, *Chem. Commun.* **2011**, *47*, 7968-7970.

[67] K. Rurack, in *Standardization and Quality Assurance in Fluorescence Measurements I, Vol. 5* (Ed.: U. Resch-Genger), Springer Berlin Heidelberg, **2008**, pp. 101-145.

[68] J. R. Casey, S. Grinstein, J. Orlowski, *Nat. Rev. Mol. Cell Biol.* **2010**, *11*, 50-61.

[69] A. P. Demchenko, *J. Fluoresc.* **2010**, *20*, 1099-1128.
[70] Catalase reacts with H_2O_2 at a rate close to the diffusion limit and was added to exclude the possibility of H_2O_2 involvement in these reactions.
[71] J. S. Beckman, W. H. Koppenol, *Am. J. Physiol. Cell Physiol.* **1996**, *271*, C1424-C1437.
[72] H. Gutfreund, *Trends Biochem. Sci* **1999**, *24*, 457-460.
[73] a) A. Sikora, J. Zielonka, M. Lopez, J. Joseph, B. Kalyanaraman, *Free Radical Biol. Med.* **2009**, *47*, 1401-1407; b) J. Zielonka, A. Sikora, J. Joseph, B. Kalyanaraman, *J. Biol. Chem.* **2010**, *285*, 14210-14216; c) A. Sikora, J. Zielonka, M. Lopez, A. Dybala-Defratyka, J. Joseph, A. Marcinek, B. Kalyanaraman, *Chem. Res. Toxicol.* **2011**, *24*, 687-697.
[74] H. Y. Lee, X. Jiang, D. Lee, *Org. Lett.* **2009**, *11*, 2065-2068.
[75] a) M. Santra, S.-K. Ko, I. Shin, K. H. Ahn, *Chem. Commun.* **2010**, *46*, 3964-3966; b) Y. Urano, M. Kamiya, K. Kanda, T. Ueno, K. Hirose, T. Nagano, *J. Am. Chem. Soc.* **2005**, *127*, 4888-4894; c) T.-H. Kim, T. M. Swager, *Angew. Chem. Int. Ed.* **2003**, *42*, 4803-4806; d) Y.-S. Cho, K. H. Ahn, *Tetrahedron Lett.* **2010**, *51*, 3852-3854; e) C. Liu, J. Pan, S. Li, Y. Zhao, L. Y. Wu, C. E. Berkman, A. R. Whorton, M. Xian, *Angew. Chem. Int. Ed.* **2011**, *50*, 10327-10329; f) H. Maeda, K. Yamamoto, Y. Nomura, I. Kohno, L. Hafsi, N. Ueda, S. Yoshida, M. Fukuda, Y. Fukuyasu, Y. Yamauchi, N. Itoh, *J. Am. Chem. Soc.* **2005**, *127*, 68-69; g) J. S. Rush, K. E. Beatty, C. R. Bertozzi, *ChemBioChem* **2010**, *11*, 2096-2099; h) M. Kamiya, Y. Urano, N. Ebata, M. Yamamoto, J. Kosuge, T. Nagano, *Angew. Chem. Int. Ed.* **2005**, *44*, 5439-5441; i) A. E. Albers, K. A. Rawls, C. J. Chang, *Chem. Commun.* **2007**, 4647-4649.
[76] a) L. F. Mottram, S. Boonyarattanakalin, R. E. Kovel, B. R. Peterson, *Org. Lett.* **2006**, *8*, 581-584; b) W.-C. Sun, K. R. Gee, D. H. Klaubert, R. P. Haugland, *J. Org. Chem.* **1997**, *62*, 6469-6475.
[77] F. Song, A. L. Garner, K. Koide, *J. Am. Chem. Soc.* **2007**, *129*, 12354-12355.
[78] A. R. Lippert, d. B. G. C. Van, C. J. Chang, *Acc. Chem. Res.* **2011**, *44*, 793-804.
[79] a) V. V. Rostovtsev, L. G. Green, V. V. Fokin, K. B. Sharpless, *Angew. Chem. Int. Ed.* **2002**, *41*, 2596-2599; b) C. W. Tornoe, C. Christensen, M. Meldal, *J. Org. Chem.* **2002**, *67*, 3057-3064.
[80] K. E. Borbas, J. I. Bruce, *Org. Biomol. Chem.* **2007**, *5*, 2274-2282.
[81] C. Wendeln, S. Rinnen, C. Schulz, T. Kaufmann, H. F. Arlinghaus, B. J. Ravoo, *Chem. Eur. J.* **2012**, *18*, 5880-5888.
[82] T. Ishiyama, M. Murata, N. Miyaura, *J. Org. Chem.* **1995**, *60*, 7508-7510.
[83] In the case of **21e** Pd^0 mediated propargyl cleavage was also observed.

[84] M. S. Tremblay, D. Sames, *Org. Lett.* **2005**, *7*, 2417-2420.
[85] D. R. Lide, *CRC Handbook of Chemistry and Physics, 83rd Edition*, CRC Press LLC, **2002**.
[86] A. R. Lippert, T. Gschneidtner, C. J. Chang, *Chem. Commun.* **2010**, *46*, 7510-7512.
[87] M. J. Selwyn, *Biochim. Biophys. Acta* **1965**, *105*, 193-195.
[88] Although the active site cystein in PTP1B can reacts with H_2O_2, the rate constant for this reaction is low (10 M^{-1} s^{-1}). It has therefore been suggested that other RONS may play a more pronounced role in its deactivation. H_2O_2 deactivation of PTP1B may only be significant in cellular compartments with low H_2O_2 clearance. See ref 9 for a discussion of this.
[89] a) C. E. Paulsen, K. S. Carroll, *Chem. Rev.* **2013**, *113*, 4633-4679; b) T. H. Truong, K. S. Carroll, *Crit. Rev. Biochem. Mol. Biol.* **2013**, *48*, 332-356.
[90] The inner filter effect is a decrease in the effective excitation power due to other absorbing compounds in solution (in this case **Eu43**)
[91] J. E. Moses, A. D. Moorhouse, *Chem. Soc. Rev.* **2007**, *36*, 1249-1262.
[92] M. Meldal, C. W. Tornoe, *Chem. Rev.* **2008**, *108*, 2952-3015.
[93] a) M. Jauregui, W. S. Perry, C. Allain, L. R. Vidler, M. C. Willis, A. M. Kenwright, J. S. Snaith, G. J. Stasiuk, M. P. Lowe, S. Faulkner, *Dalton Trans.* **2009**, 6283-6285; b) J. K. Molloy, O. Kotova, R. D. Peacock, T. Gunnlaugsson, *Org. Biomol. Chem.* **2012**, *10*, 314-322; c) P. A. Sukerkar, K. W. MacRenaris, T. R. Townsend, R. A. Ahmed, J. E. Burdette, T. J. Meade, *Bioconjug. Chem.* **2011**, *22*, 2304-2316.
[94] a) M. Suchy, R. Bartha, R. H. E. Hudson, *RSC Advances* **2013**, *3*, 3249-3259; b) Y. Song, X. Xu, K. W. MacRenaris, X.-Q. Zhang, C. A. Mirkin, T. J. Meade, *Angew. Chem. Int. Ed.* **2009**, *48*, 9143-9147; c) L.-R. L. M. De, Z. Kovacs, *Bioconjugate Chem.* **2008**, *19*, 391-402; d) F. Fernandez-Trillo, J. Pacheco-Torres, J. Correa, P. Ballesteros, P. Lopez-Larrubia, S. n. Cerdan, R. Riguera, E. Fernandez-Megia, *Biomacromolecules* **2011**, *12*, 2902-2907; e) D. E. Prasuhn, Jr., R. M. Yeh, A. Obenaus, M. Manchester, M. G. Finn, *Chem. Commun.* **2007**, 1269-1271.
[95] Z. Kovacs, A. D. Sherry, *J. Chem. Soc., Chem. Commun.* **1995**, 185-186.
[96] C. Shao, X. Wang, J. Xu, J. Zhao, Q. Zhang, Y. Hu, *J. Org. Chem.* **2010**, *75*, 7002-7005.
[97] T. R. Chan, R. Hilgraf, K. B. Sharpless, V. V. Fokin, *Org. Lett.* **2004**, *6*, 2853-2855.
[98] S. Ciampi, T. Boecking, K. A. Kilian, J. B. Harper, J. J. Gooding, *Langmuir* **2008**, *24*, 5888-5892.

[99] Z. H. Soomro, S. Cecioni, H. Blanchard, J.-P. Praly, A. Imberty, S. Vidal, S. E. Matthews, *Org. Biomol. Chem.* **2011**, *9*, 6587-6597.
[100] J. A. Gonzalez-Vera, E. Lukovic, B. Imperiali, *J. Org. Chem.* **2009**, *74*, 7309-7314.
[101] a) A. A. Kislukhin, V. P. Hong, K. E. Breitenkamp, M. G. Finn, *Bioconjugate Chem.* **2013**, *24*, 684-689; b) S. I. Presolski, V. Hong, S.-H. Cho, M. G. Finn, *J. Am. Chem. Soc.* **2010**, *132*, 14570-14576.
[102] V. Hong, S. I. Presolski, C. Ma, M. G. Finn, *Angew. Chem. Int. Ed.* **2009**, *48*, 9879-9883.
[103] G. J. Stasiuk, M. P. Lowe, *Dalton Trans.* **2009**, 9725-9727.
[104] J.-C. G. Bunzli, S. V. Eliseeva, in *Lanthanide Luminescence, Vol. 7* (Eds.: P. Hänninen, H. Härma), Springer GmbH, Springer-Verlag Berlin Heidelberg 2011, **2011**, pp. 1-46.

Acta Universitatis Upsaliensis

Digital Comprehensive Summaries of Uppsala Dissertations from the Faculty of Science and Technology 1208

Editor: The Dean of the Faculty of Science and Technology

A doctoral dissertation from the Faculty of Science and Technology, Uppsala University, is usually a summary of a number of papers. A few copies of the complete dissertation are kept at major Swedish research libraries, while the summary alone is distributed internationally through the series Digital Comprehensive Summaries of Uppsala Dissertations from the Faculty of Science and Technology. (Prior to January, 2005, the series was published under the title "Comprehensive Summaries of Uppsala Dissertations from the Faculty of Science and Technology".)

Distribution: publications.uu.se
urn:nbn:se:uu:diva-236760

ACTA
UNIVERSITATIS
UPSALIENSIS
UPPSALA
2014